

Phase diffusion and suppression of the supercurrent by quantum-mechanical fluctuations of the Josephson plasma at small superconducting point contacts

Kurt Gloos^{1,2} and Frithjof Anders¹

¹ *Institut für Festkörperphysik, Technische Universität Darmstadt, D-64289 Darmstadt, Germany*

² *Max-Planck-Institut für chemische Physik fester Stoffe, D-01187 Dresden, Germany*

(March 8, 1999)

The RCSJ model of resistively and capacitively shunted Josephson junctions is used to describe superconducting point contacts over a wide range of resistances up to the metallic – tunneling transition. Their small dynamic capacitance of order $C = 0.1$ fF due to the point-contact geometry results in a huge plasma frequency. The critical current is then strongly suppressed and the contact resistance becomes finite because of quantum-mechanical zero-point fluctuations of the Josephson plasma and the rather large escape rate out of the zero-voltage state due to quantum tunneling. We test the predictions of the RCSJ model on the classical superconductors lead, indium, aluminum, and cadmium.

I. OVERVIEW

Point contacts between two superconductors have attracted interest for a number of reasons: They can be used to study the behaviour of a macroscopic quantum object¹ as well as quantum transport when the junction consists of few atoms only^{2,3}. They may also help to extract information on the order parameter of compounds like the heavy-fermion superconductors, although those experiments are not as easy to interpret as has previously been assumed⁴.

Metallic point contacts of classical superconductors have first been investigated systematically by Muller *et al.*^{5–8}. They observed that, on reducing the contact area, the residual contact resistance R_0 at zero bias becomes finite and the critical current I_c smaller than the theoretical value I_c^0 at a temperature $T \ll T_c$ even when the normal-state resistance $R_N = R(T > T_c)$ is far below the quantum limit $R_K/2 = h/2e^2 = 12.9$ k Ω . This was attributed to the presence of electrical radio-frequency noise and additional damping of the junctions at high frequencies due to the small impedance (that is the large capacitance) of the current and voltage leads^{7,8}. The Andreev-reflection excess current, on the other hand, was found not to depend on the lateral size of the junctions.

We show here that the behaviour of those Josephson junctions can better be described by the small capacitance C typical for the three-dimensional point-contact geometry. Taking into account the capacitance of the junctions as an adjustable parameter, we derive relations between R_N and the residual resistance R_0 as well as the product $R_N I_c$, and estimate both the plasma frequency ω_p and the Josephson coupling energy E_{JE} from the current-voltage $I(U)$ characteristic at $I \rightarrow 0$. Our experiments on the classical superconductors lead, indium, aluminum, and cadmium fit the predictions fairly well. Using the horizon model, the capacitance C can be traced back to the properties of vacuum tunneling junctions in the normal state.

II. THEORY

The system of Cooper pairs in a bulk sample forms one wavefunction $\Psi = |\Psi_0| \exp(i\varphi)$. The gradient of the phase φ drives the current. According to B. D. Josephson⁹, by coupling two superconductors weakly to each other using a thin insulating layer between them, the phase difference $\varphi := \varphi_2 - \varphi_1$ across the junction results in a supercurrent

$$I = I_c^0 \sin \varphi \quad (1)$$

as long as the voltage drop U is much smaller than the superconducting energy gap $2\Delta(T)/e$. According to Ambegaokar and Baratoff¹⁰ the critical current of a Josephson tunnel junction $I_c^0 = (\pi\Delta/2eR_N) \tanh(\Delta/2k_B T)$.

The critical current through short metallic junctions between isotropic BCS-type superconductors was derived by Kulik and Omel'yanchuk to be (KO1) $I_c^0 = (1.32 \pi\Delta/2eR_N) \tanh(\Delta/2k_B T)$ ¹¹ in the dirty limit (electron mean free path l much shorter than the superconducting coherence length ξ), and (KO2) $I_c^0 = (\pi\Delta/eR_N) \tanh(\Delta/2k_B T)$ ¹² in the clean limit $l \gg \xi$. We will see below that quantum fluctuations of the Josephson plasma can further reduce the critical current. The superscript 0 denotes then the above intrinsic value.

The current-phase relationship of a metallic Josephson junction in the clean limit deviates from the simple sinusoidal of a tunnel junction. It depends on the transmission coefficient D as¹³

$$I(\varphi) = \frac{\pi\Delta}{2eR_N} \frac{\sin\varphi}{\delta} \tanh\left(\frac{\Delta\delta}{2k_B T}\right) \quad (2)$$

with $\delta = \sqrt{1 - D \sin^2(\varphi/2)}$. The normal-state contact resistance in the ballistic limit

$$R_N = \frac{2R_K}{(ak_F)^2} D^{-1} \quad (3)$$

Here k_F is the Fermi wave number and a the contact radius. By varying the transmission coefficient, the junction can be tuned from pure metallic ($D = 1$) to pure tunnel ($D = 0$) behaviour.

Note the effects we are going to investigate do not involve an 'energy cost' due to lateral confinement that could suppress the superconducting features in the contact region: although the junctions are rather small – with a typical metallic $k_F \approx 15 \text{ nm}^{-1}$ a $R_N = 100 \Omega$ junction has a contact radius a of about 2 nm – the Heisenberg uncertainty principle yields a spread with respect to momentum, and not one with respect to energy.

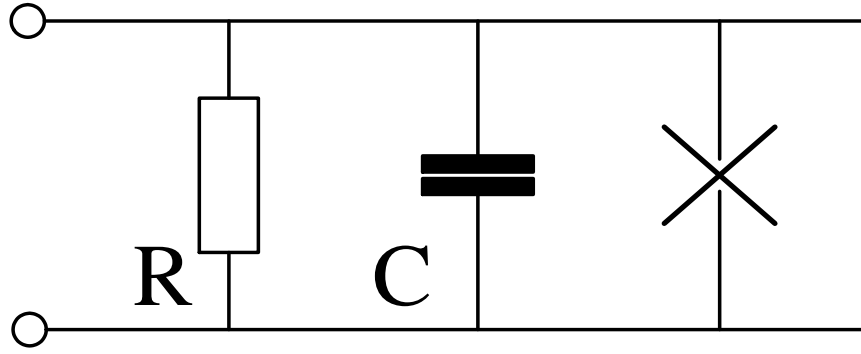


FIG. 1. RCSJ model. The junction itself is represented by \times . The current is applied to and the voltage detected at the terminals denoted by \circ .

A. The RCSJ model and the quasi-particle resistance

When the applied voltage $U = 0$, the phase does not change because $\dot{\varphi} = \partial\varphi/\partial t = 2eU/\hbar = 0$, and the current through the junction is constant⁹. If the voltage is finite, the phase increases at a rate $2eU/\hbar \approx 3 \cdot 10^{15} (1/s) \cdot U(V)$, and the current has an oscillatory component at extremely high frequencies. D. E. McCumber¹⁴ and W. C. Stewart¹⁵ took into account that besides the supercurrent across the Josephson tunnel junction there exist also a normal quasi-particle current, described by a parallel resistance $R = R_{qp}$, as well as a displacement current due to a (stray) capacitance C (Fig. 1). This capacitance is important for the properties of the junction because it represents a short circuit for the high-frequency part of the supercurrent. The total current of such a resistively and capacitively shunted junction (RCSJ) is $I = I_c^0 \sin\varphi + U/R_{qp} + CdU/dt$ or

$$\frac{I}{I_c^0} = \sin\varphi + \frac{\dot{\varphi}}{\omega_c} + \frac{\ddot{\varphi}}{\omega_p^2} \quad (4)$$

with the plasma frequency $\omega_p = \sqrt{2eI_c^0/\hbar C}$ and the characteristic frequency $\omega_c = 2eI_c^0 R_{qp}/\hbar$.

The quasi-particle resistance $R = R_{qp}$ is *a priori* unknown. Generally, it will depend both on voltage, on current, or on phase. Above T_c , without Josephson effect, the quasi-particle resistance equals just the normal-state contact resistance R_N , originating purely from the quasi-particle current through the junction (we assume there is no external shunt resistance). For a tunnel junction, this R_{qp} is proportional to the square modulus of the tunnel matrix element. For a ballistic junction, like the ones we are using, R_{qp} involves an infinite resummation of multiple quasi-particle transmissions through the contact. Then, energy is not dissipated at the junction itself: electrons equilibrate far away from the junction in the bulk metal. By including non-linear effects like quasi-particle quasi-particle interactions or

electron-phonon coupling, the contact resistance, and thus R_{qp} , depends on temperature and the applied bias voltage U .

Below T_c , the situation changes completely as a Josephson supercurrent can flow through the junction. However, well below T_c there is no quasi-particle density of states within the energy gap 2Δ on both sides of the junction. Therefore, $R_{\text{qp}} \rightarrow \infty$ for an ideal junction at low bias voltage $|U| \ll \Delta/e$. At a Josephson tunnel junction, R_{qp} can be directly observed by suppressing the supercurrent using a small magnetic field less than the critical field. Tunnel experiments have shown that the damping resistance can be much smaller than the intrinsic quasi-particle resistance R_{qp} , see for example Ref.¹. This is probably due to parasitic damping of the high-frequency electromagnetic field generated at the junction.

The quasi-particle resistance of a metallic Josephson junction (or point contact) can not be measured directly, as far as we know. But it seems plausible, to apply the same arguing as for the tunnel junctions: For a clean BCS-type superconductor far below T_c , the quasi-particle density of states has vanished in the vicinity of the chemical potential, and therefore the intrinsic $R_{\text{qp}} \rightarrow \infty$. Recently, Levy Yeyati *et al.*³ derived the dissipative part of the current through a superconducting quantum point contact, that is a ballistic junction with one conducting channel. Assuming the same relation to hold also in the general case of a ballistic Josephson junction, the inverse quasi-particle resistance

$$R_{\text{qp}}^{-1}(\varphi) = \frac{D}{R_N} \frac{\pi \Delta^2}{16 \Gamma k_B T} \left[\frac{\sin \varphi}{\delta} \operatorname{sech} \left(\frac{\Delta \delta}{2 k_B T} \right) \right]^2 \quad (5)$$

$\Gamma = \hbar/\tau$ being the inelastic relaxation rate, and τ the quasi-particle lifetime. Most importantly, the dissipative part of the current vanishes at $\varphi \rightarrow 0$ or at $I \ll I_c$, that is $R_{\text{qp}} \gg R_N$.

In both type of experiments, Josephson tunnel junctions as well as metallic Josephson point contacts, there can be damping due to the external circuitry. The amount of this parasitic damping can not be predicted theoretically, because it depends on the specific experimental setup. Thus the damping resistance $R = R_{\text{qp}}$ of the RCSJ model has to be treated as a free parameter, like the capacitance, that has to be extracted from the properties of the junctions. The normal-state contact resistance may represent some lower bound of the intrinsic quasi-particle resistance, and R_N may thus serve as a first guess for the damping resistance. But otherwise there is no reason to set $R_{\text{qp}} = R_N$.

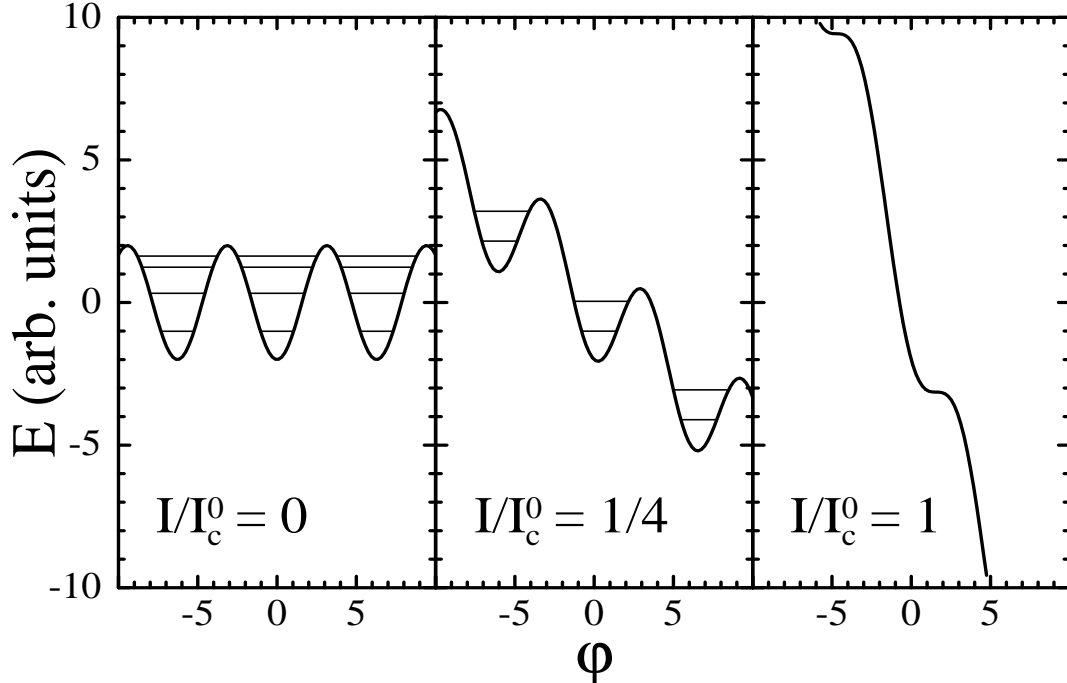


FIG. 2. Washboard potential $E(I, \varphi)$ of Eq. 6 for different values of the applied current.

Eq. 4 describes the motion of a particle with 'mass' $(\hbar/2e)^2 C$ exposed to a viscous damping force $(\hbar/2e R_{\text{qp}}) \dot{\varphi}$ in the potential

$$E(I, \varphi) = -\frac{\hbar}{2e} I \varphi - E_{\text{JE}} \cdot \cos \varphi \quad (6)$$

$E_{\text{JE}} = \hbar I_c^0 / 2e$ is called Josephson coupling energy. The potential Eq. 6 has the shape of a washboard, its wells have a depth of $2E_{\text{JE}}$ at $I = 0$ (Fig. 2). The number of discrete energy levels in these wells amounts to about¹ $\text{Int}(2E_{\text{JE}}/\hbar\omega_p)$. The lowest one is the zero-point energy $\epsilon_0 = \hbar\omega_p/2$. Minima exist as long as $I < I_c^0$, and the static solution of Eq. 4 is $I/I_c^0 = \sin\varphi$. If the time constant $R_{\text{qp}}C$ is much smaller than the period of the plasma oscillations, the system is overdamped. The only stable state is then at such a potential minimum and the $I(U)$ - characteristic is non-hysteretic. An underdamped junction can either be at a minimum, the supercurrent flowing without a voltage drop. Or it can run down the washboard, and the current is accompanied by a voltage. The $I(U)$ - characteristic is then hysteretic. At $I > I_c^0$ there are no more minima, and the system is definitely in the resistive state with $\dot{\varphi} \neq 0$.

The RCSJ model has been applied to weakly damped planar tunnel junctions (with an insulating oxide layer instead of a vacuum gap) of classical superconductors like niobium and tin: Fulton and Dunkleberger¹⁶ observed thermally activated escape from the minima, Voss and Webb¹⁷ and later on Washburn *et al.*¹⁸ reported macroscopic quantum tunneling through the wells of the washboard potential. Its discrete energy levels have been observed by Martinis *et al.*¹⁹. Obviously, the RCSJ model is the minimum system to study the Josephson effect at solitary point contacts.

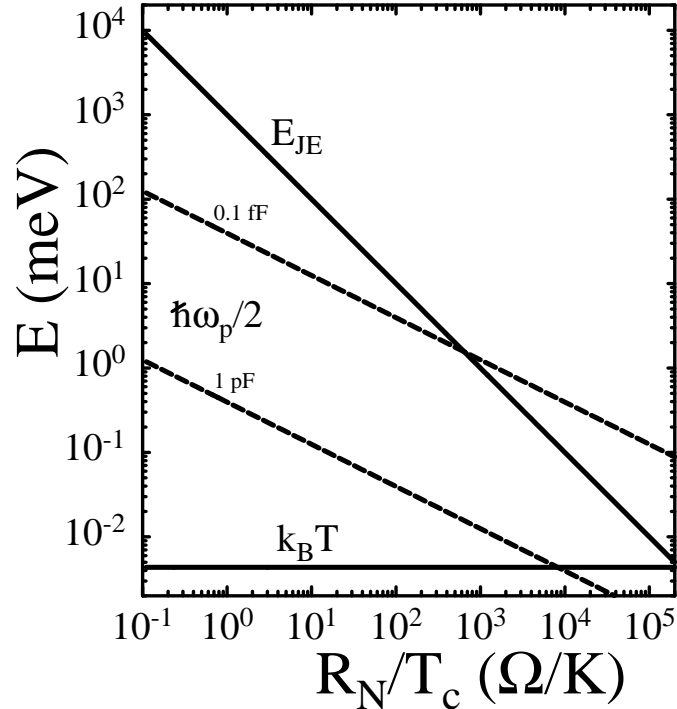


FIG. 3. Josephson coupling energy E_{JE} , zero-point energy $\hbar\omega_p/2$ at two different capacitances C , and thermal energy $k_B T$ at 50 mK vs. R_N/T_c of junctions between BCS-type superconductors in the clean limit.

Let us illustrate the situation by setting in numbers. For junctions with BCS-type superconductors in the clean limit the coupling energy amounts to

$$E_{\text{JE}} \approx 1 \text{ eV} \frac{T_c(\text{K})}{R_N(\Omega)} \quad (7)$$

at a zero-point energy of the Josephson plasma

$$\frac{\hbar\omega_p}{2} \approx 12 \text{ meV} \sqrt{\frac{T_c(\text{K})}{R_N(\Omega)C(\text{fF})}} \quad (8)$$

Planar tunnel junctions typically have capacitances of order 1 pF. For them $\hbar\omega_p/2$ can be orders of magnitude smaller than E_{JE} . To induce a detectable escape from the minima of the potential wells, these junctions have to be driven near the critical current. Metallic point contacts, on the other hand, have considerably smaller capacitances. They are believed to be of order 1 fF⁸. And although the coupling energy can be much larger than the thermal energy $k_B T$ (about 4 μeV at our lowest temperature of ~ 50 mK), the zero-point energy can be quite high, see Fig. 3. This has direct consequences with respect to the critical current and the residual resistance, because in such a system

the particle can escape easily from the minima even at small currents, accompanied by 2π phase slips. In addition, because of the quality factor

$$Q = \omega_p R_{qp} C \approx 0.04 R_{qp}(\Omega) \sqrt{\frac{T_c(K)C(\text{fF})}{R_N(\Omega)}} \quad (9)$$

those metallic junctions have to be expected to be in the cross-over region between weak and strong damping, if the quasi-particle resistance R_{qp} was of the same size as the normal-state resistance R_N .

B. Critical current suppressed by quantum fluctuations

The quantum-mechanical treatment of the particle in the washboard potential describes the phase as an operator conjugated to the charge $q = 2e$ of the Cooper pairs, $[\varphi, q] = 2ie$. This allows to include quantum fluctuations and phase diffusion. The macroscopic voltage is then given by the time derivative of the expectation value of the phase $U = (\hbar/2e)\partial\langle\varphi(t)\rangle/\partial t$. It was shown, for example, that Josephson junctions at $T = 0$ can undergo a phase transition from the superconducting to the resistive state, depending on the strength of dissipation or damping²⁰.

A current $I = xI_c^0$ tilts the washboard potential (Fig. 2) and reduces both the minimum height of the wells¹⁶

$$2E(x) = E_{JE} [x(2 \arcsin x - \pi) + 2 \cos \arcsin x] \quad (10)$$

and the plasma frequency

$$\omega(x) = \omega_p (1 - x^2)^{1/4}. \quad (11)$$

I_c can closely approximate I_c^0 at small R_N when $\hbar\omega_p \ll E_{JE}$. The $I(U)$ -characteristic shows then a sudden rise at $I \approx I_c^0$. At larger resistances, E_{JE} decreases faster than $\hbar\omega_p$, and the ratio $\hbar\omega(x)/E(x)$ diverges as $x \rightarrow 1$, that is at $I \rightarrow I_c^0$. Assuming the supercurrent being suppressed by the quantum-mechanical fluctuations of the Josephson plasma, the actual critical current I_c of the RCSJ model less than I_c^0 is reached at

$$2E(x_c) \approx \hbar\omega(x_c)/2 \quad (12)$$

when the lowest energy level coincides with the minimum height of the potential well. The phase difference across the junction is then not well-defined any more. Eq. 12 makes the reduced critical current $x_c = I_c/I_c^0$ an implicit function of the intrinsic I_c^0 and of the capacitance via

$$I_c^0 \approx \frac{\pi e}{R_K C} \left[\frac{E_{JE}\omega(x_c)}{\omega_p E(x_c)} \right]^2. \quad (13)$$

Because of the quantum fluctuations the $I(U)$ - characteristic is washed out and also the critical current becomes less well defined.

Eq. 13 relates the normal-state resistance of a junction to its reduced critical current x_c as

$$R_N(x_c) \approx R_K(R_N I_c^0) \frac{C}{\pi e} \left[\frac{\omega_p E(x_c)}{E_{JE}\omega(x_c)} \right]^2 \quad (14)$$

depending only on the capacitance C and the material-dependent parameter $(R_N I_c^0)$. The supercurrent vanishes completely above

$$R_N(x_c = 0) \approx R_K(R_N I_c^0) \frac{C}{\pi e}. \quad (15)$$

Although we have neglected damping, Eq. 15 resembles the $s = \sqrt{4R_K C I_c^0 / e\pi} = 1.5$ and $\eta = R_K / 8\pi R_{qp} = 1/(2\pi)$ fixpoint for the localization – delocalization transition at $T \rightarrow 0$, the so-called Schmid transition²⁰. It demonstrates that our simple physical argument captures the essence of a renormalisation group calculation.

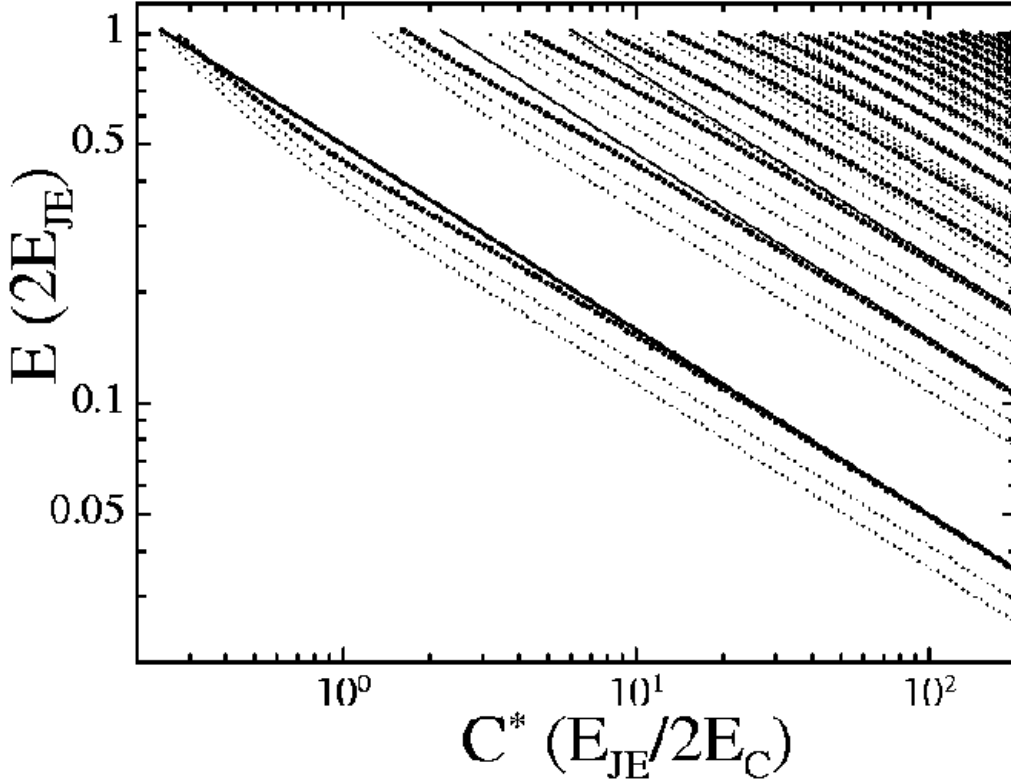


FIG. 4. Energy of the stationary states in units of $2E_{JE}$ vs. reduced mass $C^* = E_{JE}/2E_C$ for tunnel junctions ($D = 0$) and metallic junctions ($D = 1$) at low ($T/T_c = 0.01$) and high ($T/T_c = 0.1$) temperatures (from top to bottom). The analytical zero-point energy $\epsilon_0 = 2E_{JE}\sqrt{E_C/2E_{JE}}$ as well as the first and second excited level (solid lines) fit well the numerical data for the tunnel junctions ($E_C = e^2/2C$).

A metallic Josephson junction with finite transmission coefficient slightly changes the situation with respect to a tunnel junction. Neglecting dissipation, the Schrödinger equation

$$\frac{\partial^2}{\partial \varphi^2} \Psi = \frac{C}{2e^2} [E(\varphi) - \epsilon] \Psi \quad (16)$$

can be solved numerically. Fig. 4 shows the Eigen energy $\epsilon = \epsilon_i$ of the stationary states $i = 0, 1, 2, \dots$ fit quite well the analytical data of the washboard potential Eq. 6 at small energies. For metallic junctions with the current-phase relationship of Eq. 2, the potential minima broaden and the levels shift towards smaller energies. Since these are small corrections, for ease of use, and because we do not know the transmission coefficient of the individual junctions, our discussion will be based on the washboard potential.

For $R_N I_c^0 \approx 0.1 \text{ meV}$ and $C \approx 1 \text{ fF}$ the critical resistance of Eq. 15 is of order $5 \text{ k}\Omega$, which is still in the metallic regime. It shows that these phenomena due to the capacitance of the junctions have to be taken into account seriously.

C. Phase diffusion: Finite contact resistance and suppression of the critical current

At sufficiently high temperatures thermal activation induces escape from the potential minima by 2π phase slips, that is the phase diffuses. In this regime, the finite contact resistance due to a small capacitance has already been discussed by Ambegaokar and Halperin²¹.

At $T \rightarrow 0$ escape from the potential wells is mainly due to quantum tunneling. The tunneling rate has the form, see for example Refs.^{22,23},

$$\Gamma_{QT} = A \exp(-B) . \quad (17)$$

In WKB approximation and neglecting damping, the coefficients

$$A = A_0 \frac{2\epsilon_0}{\hbar} \sqrt{\frac{B}{2\pi}} \quad (18)$$

and

$$B = \frac{1}{e} \int \sqrt{C [E(\varphi) - \epsilon_0]} d\varphi. \quad (19)$$

The integral runs over that phase space in which $E(\varphi) > \epsilon_0$. The parameter $A_0 = \sqrt{60}$ for the cubic potential of Refs. ^{22,23}. (We did not succeed in deriving A_0 , but we hope that it does not depend strongly on the shape of the potential). We have estimated the coefficients A and B both for tunnel and metallic junctions (Fig. 5). Neglecting the exact shape of the washboard potential, both A and B may be overestimated by about 20 per cent. In the tunneling rate these corrections partly compensate. Our numerical results strongly deviate from the analytical form when the mass becomes small. The zero-point energy is then quite high, the effective potential the particle has to tunnel through becomes small, and the WKB approximation breaks down.

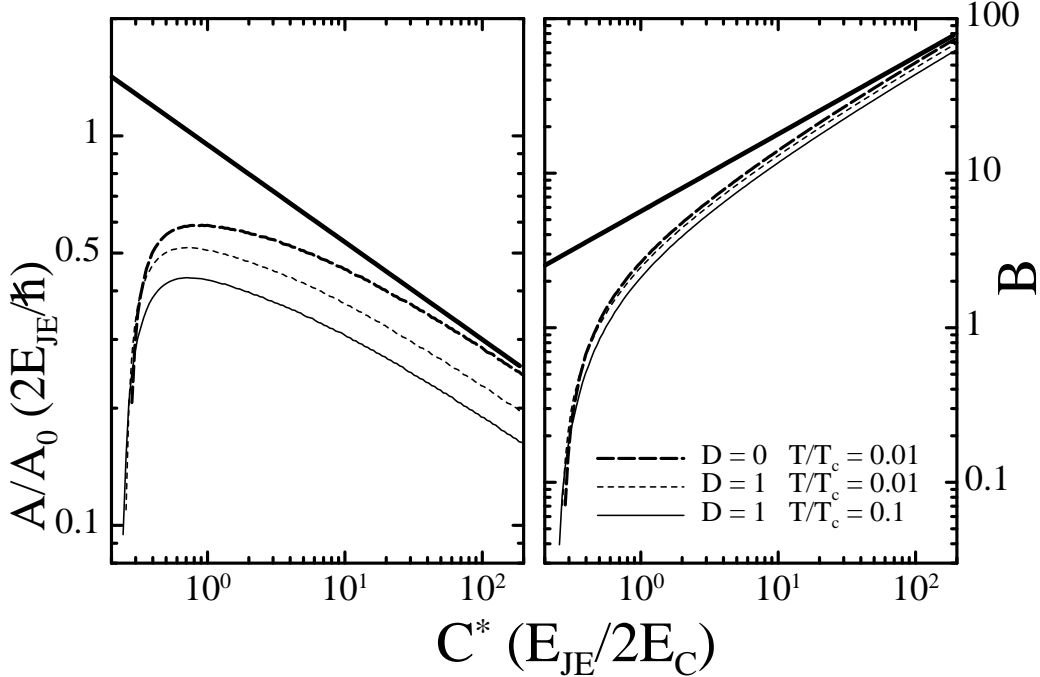


FIG. 5. a) A/A_0 and b) B vs. reduced mass $C^* = E_{JE}/2E_C$ for tunnel junctions ($D = 0$) and metallic junctions ($D = 1$) at low ($T/T_c = 0.01$) and high ($T/T_c = 0.1$) temperatures. The analytical $A/A_0 = 2\epsilon_0\sqrt{B/2\pi}/\hbar$ and $B = \sqrt{16E_{JE}/E_C}$ (solid lines) fit well the numerical data of the tunnel junctions at large masses.

Caldeira and Leggett²² and Larkin *et al.*²³ derived the rate

$$\Gamma_{QT} = \gamma \frac{\omega_p}{2\pi} \exp \left(-\frac{14.4E_{JE}}{\hbar\omega_p} \left[1 + \frac{0.87}{Q} + \dots \right] \right) \quad (20)$$

with $\gamma \approx \sqrt{120\pi(14.4E_{JE}/\hbar\omega_p)}$ for tunneling out of a cubic potential. Eq. 20 holds exactly at weak damping, when the quality factor $Q \gg 1$. The tunneling rate is considerably reduced at strong damping $Q \ll 1$. In what follows, and for ease of calculation, we assume the junctions are only weakly damped by including the term linear in $1/Q$.

Note that for the sinusoidal current-phase relation and the washboard potential (that is for $I \ll I_c$) the prefactor in the exponent is not 14.4 as for the cubic potential (that is for $I \approx I_c$) but $8\sqrt{2} \approx 11.3$. Since this is also a small correction, like for the A and the B coefficients mentioned above, we will discuss our experimental results using the above tunneling rate Eq. 20. This also has the advantage of including possible corrections due to damping.

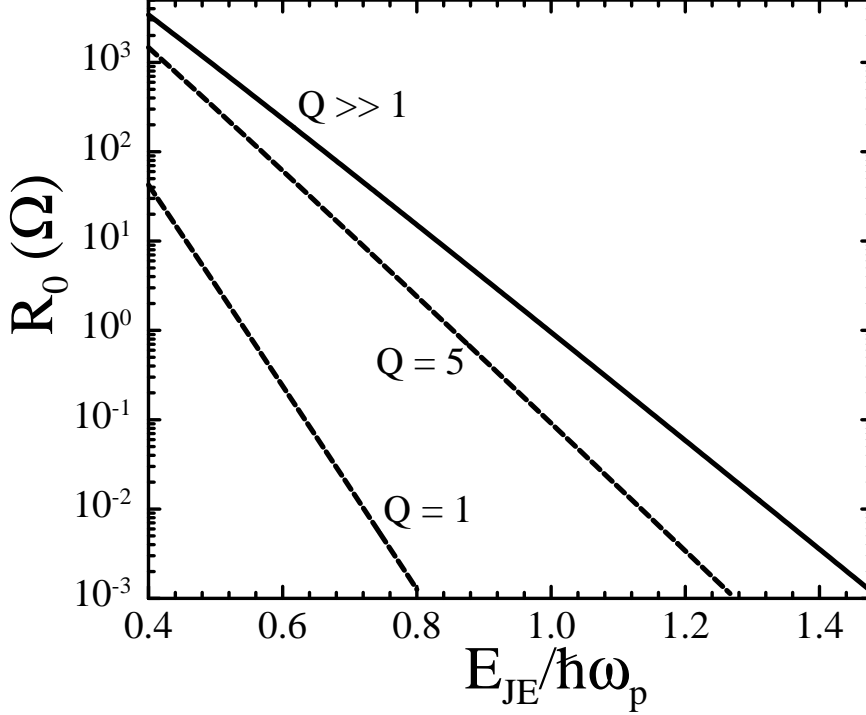


FIG. 6. Residual resistance R_0 vs. $E_{JE}/\hbar\omega_p$ at weak damping $Q \gg 1$, $Q = 5$, and $Q = 1$.

The asymmetry of the washboard potential due to a current flow yields a net phase slip rate $\dot{\phi}$, that is the phase drifts. Tilting the potential enhances the tunneling rate exponentially. Following Tinkham's discussion²⁴ we get for the RCSJ model and Eq. 20 at weak damping

$$\dot{\phi}(x) \approx 4\pi\Gamma_{QT} \sinh\left(\frac{7.2\pi x E_{JE}}{\hbar\omega_p} \left[1 + \frac{0.87}{Q}\right]\right). \quad (21)$$

Here we have used $E(x) \approx E_{JE}(1 - \pi x/2)$ and $\omega(x) \approx \omega_p$, a good approximation as long as $x = I/I_c^0 \leq 0.5$. The phase slips result in a voltage drop $U = \hbar\dot{\phi}/2e$. Consequently the differential resistance

$$dU(I)/dI \approx R_0 \cosh\left(\frac{3.6\pi}{e\omega_p} I \left[1 + \frac{0.87}{Q}\right]\right) \quad (22)$$

with the residual resistance $R_0 = dU/dI(I = 0)$

$$R_0 \approx 1.8\gamma R_K \left[1 + \frac{0.87}{Q}\right] \exp\left(-\frac{14.4E_{JE}}{\hbar\omega_p} \left[1 + \frac{0.87}{Q}\right]\right). \quad (23)$$

At $Q \gg 1$ one can directly read off the $E_{JE}/\hbar\omega_p$ -ratio from R_0 in Fig. 6. At strong damping, the phase becomes more localized and R_0 being strongly reduced. The second-order approximation of Eq. 22

$$\frac{dU(I)}{R_0 dI} \approx 1 + 2 \left[1 + \frac{0.87}{Q}\right]^2 \left(\frac{1.8\pi I}{e\omega_p}\right)^2 \quad (24)$$

allows to derive the plasma frequency ω_p and, through R_0 , the coupling energy E_{JE} from the $I(U)$ - characteristic at $I \ll I_c^0$. In this approximation neglecting damping means to underestimate the plasma frequency by a factor of $[1 + 0.87/Q]$. The derivation of the Josephson coupling energy, on the other hand, is barely affected by damping because the correction factors almost cancel each other.

To ensure tunneling from the lowest oscillator level at $\hbar\omega_p/2$, the tilt of the washboard potential $\hbar I/2e$ per period must be less than the energy difference of about $\hbar\omega_p$ between the two lowest levels. At $I \geq I_Z = e\omega_p/\pi$ quantum tunneling populates the second level, enhancing the total tunneling rate. This may be called Zener tunneling of the

phase. And because the phase diffuses faster than described by Eq. 21, the differential resistance should increase much stronger stronger than predicted by Eq. 22.

The supercurrent is suppressed as soon as the phase diffuses or drifts faster than ω_p or at

$$1.8 \left[1 + \frac{0.87}{Q} \right] R_K \leq R_0 \sinh \left(\frac{3.6\pi}{e\omega_p} I \left[1 + \frac{0.87}{Q} \right] \right) . \quad (25)$$

This relates the critical current

$$I_c = \frac{I_Z}{3.6 [1 + 0.87/Q]} \operatorname{arcsinh} \left(1.8 \left[1 + \frac{0.87}{Q} \right] \frac{R_K}{R_0} \right) \quad (26)$$

with the residual resistance and the plasma frequency. Here we have assumed that the Q-factor does neither depend on I nor on U . At $Q \gg 1$ the critical current is larger than I_Z as long as $R_0 < 1.8R_K / \sinh(3.6) \approx 2.6 \text{ k}\Omega$. Eq. 26 represents an upper limit for I_c because of neglecting Zener tunneling. Note that this equation is valid only when the actual critical current has been reduced already, that is at $x_c \leq 0.5$, while Eq. 13 represents a maximum for all x .

An estimate like in the previous section for the critical current yields for a $R_N = 1 \text{ k}\Omega$ junction a coupling energy of $E_{JE} \approx 0.2 \text{ meV}$ and a plasma frequency of $\omega_p \approx 0.57 \text{ (ps}^{-1})$. Neglecting damping, the residual resistance due to phase diffusion Eq. 23 amounts then to $R_0 \approx 0.92 \text{ k}\Omega$. Because of the exponential dependence in Eq. 23, a $R_N = 100 \Omega$ junction has a tiny $R_0 \approx 58 \mu\Omega$ only. Thus the residual resistance rises steeply within a very narrow resistance range.

D. Bloch-wave oscillations

To add a charge q to the capacitance C of the junction requires the Coulomb charging energy $E_C = q^2/2C$. When $E_C \geq E_{JE}$, both phase and charge do no longer behave as classical variables, but like operators. Because of the periodic washboard potential (Eq. 6) the Josephson junction can then be described using Bloch waves^{23,25}. Their wave number is the quasi charge $k = q/2e$. For a review see Ref.²⁶.

Bloch-wave oscillations represent the periodic transfer of discrete Cooper pairs across the junction, which is recharged by the external current source at a radial frequency of $\pi I/e$. These wave packages travelling in φ space of the tilted washboard potential have a finite 'momentum' $\langle \partial\varphi/\partial t \rangle$. This implies a voltage drop, and the contact resistance becomes finite. Theory predicts a region at finite bias current in which Bloch waves contribute negatively to the differential resistance^{23,25}, but the details of the spectra are difficult to derive unless the junctions are in the $E_C \gg E_{JE}$ limit. Since Bloch waves are suppressed by fluctuations, the quasi-particle resistance, that is the resistance R_{qp} of the RCSJ model, must be larger than about $R_K/4 \approx 6.4 \text{ k}\Omega$. It is therefore unlikely to observe them at metallic junctions if the quasi-particle resistance had the magnitude of R_N . Intraband transitions can be induced when the external current is strong enough. This Zener tunneling of the quasi-charge requires $I \geq e\omega_p/\pi$, like for Zener tunneling of the phase, see the previous section.

There are only few experimental reports on Bloch-wave oscillations at Josephson junctions, e. g. Ref.²⁷. In those experiments Bloch oscillations have been identified by a systematic coincidence between structures of the $I(U)$ - characteristic at certain applied DC currents and the frequency of an external microwave excitation.

E. Andreev reflection

Additional information on the properties of the junction comes from Andreev reflection at finite voltages. If the potential difference is $|U| > \Delta/e$, quasi-particles from one side of the junction can enter the other one by Andreev reflection, and return a quasi-hole. At high bias voltages this additional hole or excess current amounts to $I_{ex} = 8\Delta/3eR_N$ and $I_{ex} = (\pi^2 - 4) \Delta/4eR_N$ in the clean and the dirty limit, respectively^{28,29}.

If $|U| < \Delta/e$ the quasi-hole returns at an energy still inside the gap, and it is reflected again as a quasi-particle. Since the charge carriers gain an energy $e|U|$ per crossing the junction, $M = 2\Delta/e|U|$ ($M = 1, 2, 3, \dots$) successive reflections are required to overcome the gap. At $|U| = 2\Delta/eM$ the conductance increases stepwise. This multiple Andreev reflection becomes more pronounced at the presence of normal quasi-particle reflection at the interface, that is at $D < 1$. Normal quasi-particle reflection strongly reduces the excess current, because both the quasi-particle and the quasi-hole have to cross the interface.

The Andreev-reflection excess current can also be reduced due to a finite quasi-particle lifetime τ . For normal-superconducting junctions, lifetime effects are taken into account by the modified BTK theory³⁰, applying the Dynes'

model. At superconducting junctions, lifetime effects are expected to suppress structures due to multiple Andreev reflection, see for example Refs.^{2,3}.

As soon as phase diffusion becomes efficient and R_0 finite, it can be difficult to distinguish clearly between the Josephson supercurrent and the Andreev-reflection hole current. At large voltages $|U| \gg \Delta/e$ and beyond the critical current, however, the Andreev-reflection process is not affected by the capacity of the RCSJ model. Therefore the literature value of I_{ex} has to be expected. This has been verified previously on normal-superconducting junctions³¹.

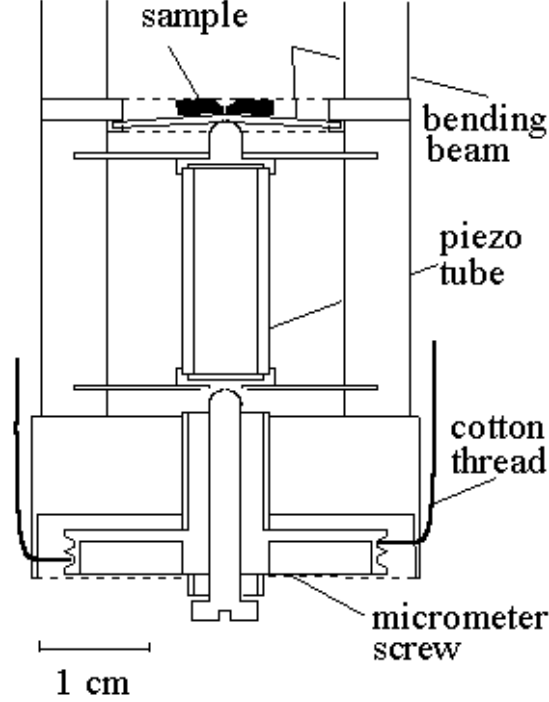


FIG. 7. Our break-junction device. The sample is broken by turning the micrometer screw using two flexible cotton threads. This screw is also used for coarsely adjusting the contact. Fine adjustment is achieved by applying a voltage at the piezo tube.

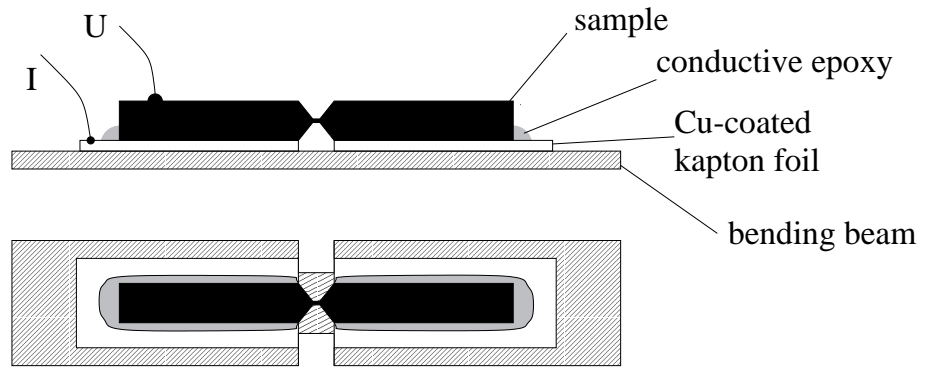


FIG. 8. The sample on the bending beam. This gold-plated beam is cut from copper alloy. Only one of the current and one of the voltage leads are shown.

III. EXPERIMENT

We prepared metallic point contacts between two bulk pieces of the BCS-type superconductors lead ($T_c = 7.2$ K), indium (3.4 K), aluminum (1.15 K), and cadmium (0.54 K) using mechanical-controllable break junctions. Fig. 7 shows our setup and Fig. 8 the sample on the bending beam. The samples, ~ 1 mm diameter wires, were broken at a predefined notch in the ultra-high vacuum region of the cold refrigerator. This avoids oxidation of the interfaces and ensures the junctions to consist of pure metal. The lateral contact size and, thus, the normal-state resistance could be adjusted in situ by a micrometer screw, driven mechanically by a pulley-and-rope and a piezo tube. The current-voltage characteristic and the differential resistance were recorded in the standard four-terminal mode with current biasing.

Twisted pairs of wires are used for the current and voltage leads. They are properly shielded. Simple LRC filters at the mixing chamber protect the sample from low-frequency (\sim MHz) noise. We have no copper-powder filter as described in Refs.^{5–8}.

We start the experiments with the contact resistance set to about $1 - 3$ m Ω at room temperature. This corresponds to a contact radius of about 10 μ m. The residual resistance ratio of the material in the contact region was then observed if possible while cooling down. We obtained as lower bound of the electronic mean free path $l \geq 70$ nm (Pb), 310 nm (In), 545 nm (Al), and 75 nm (Cd). The junctions investigated here have $R_N \geq 1$ Ω . They are therefore ballistic and have, according to Sharvin's resistance formula³², that is Eq. 3 at $D = 1$, a contact area of about $665 \text{ nm}^2 / R_N (\Omega)$. The bulk samples had residual resistance ratios of about 7570 (Pb), 4760 (In), 1270 (Al), and 1430 (Cd). This corresponds to electronic mean free paths of about 18 μ m (Pb), 29 μ m (In), 19 μ m (Al), and 12 μ m (Cd). Unless otherwise specified, the following experimental data have been obtained at low temperatures of $T \approx 50$ mK.

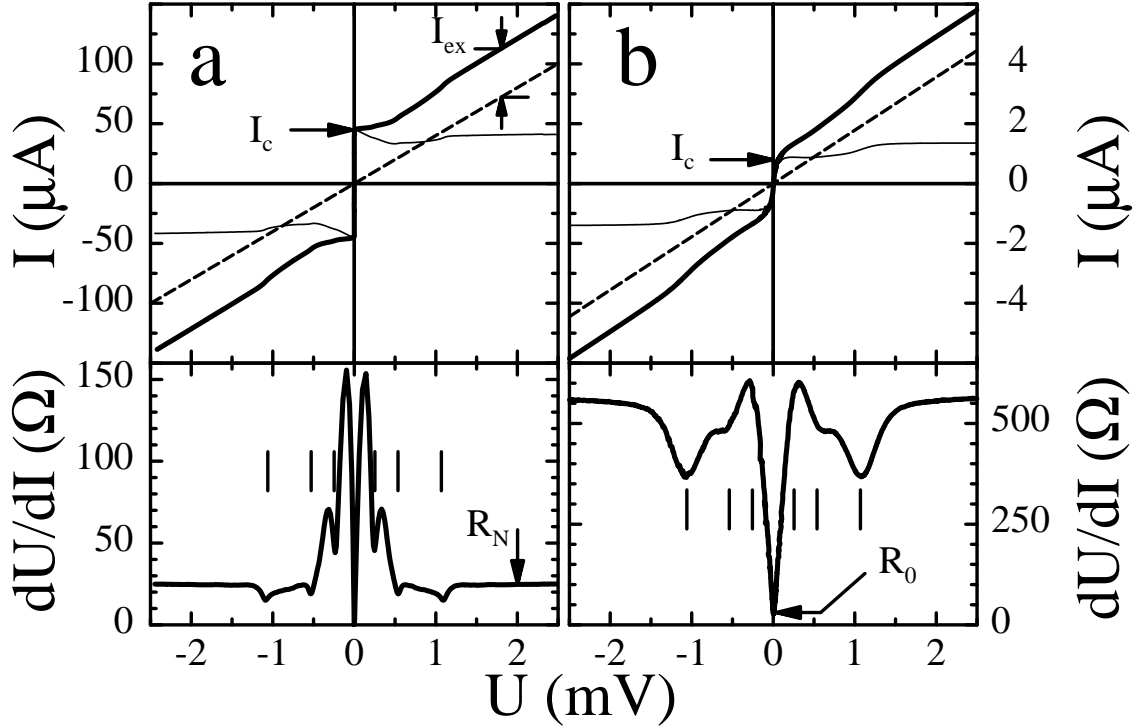


FIG. 9. I vs. U and dU/dI vs. U of a) a low-resistance and b) a high-resistance In junction at $T = 50$ mK (thick solid lines). Arrows define the various parameters used. The vertical bars mark the superconducting energy gap $2\Delta/e$ and its subharmonics. The dashed lines are the normal-state $I(U)$ characteristics. The thin solid lines represent the additional current due to the Josephson effect and the Andreev-reflection excess current.

IV. RESULTS AND DISCUSSION

The $I(U)$ - characteristics as well as the differential resistance dU/dI could be recorded over the full superconducting anomaly without excessive heating for junctions with $R_N \geq 1$ Ω . Few junctions with $R_N \approx 1 - 10$ Ω were hysteretic, either due to heating or, according to the RCSJ model, due to being weakly damped. The self-magnetic field at the

junctions could also contribute to hysteresis, but this has to be expected at much smaller contact resistances $R_N \ll 1 \Omega$. For those hysteretic junctions the critical current was extracted from that branch of the $I(U)$ - characteristic with increasing current.

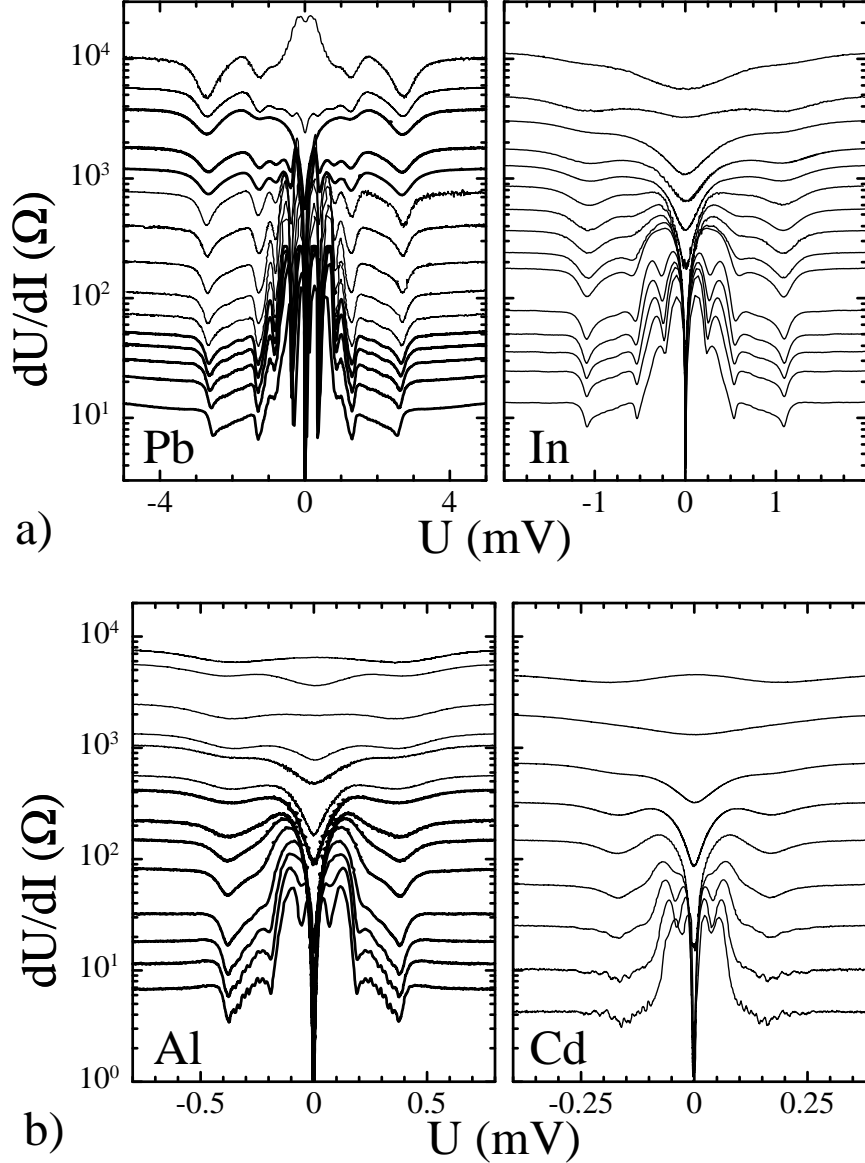


FIG. 10. Typical spectra dU/dI vs. U of a) Pb and In and b) Al and Cd junctions at $T = 50$ mK.

Fig. 9 shows two typical $I(U)$ - characteristics and dU/dI vs. U spectra as example and for defining the various parameters. A number of selected spectra are shown in Fig. 10. They look quite similar for all four superconductors. There are distinct structures due to superconductivity at small R_N , including an unresolvably small R_0 . These structures diminish at larger resistances, but their positions on the voltage axis do barely change. Finally, in the resistance range around $10 \text{ k}\Omega$ we observe, as expected, the transition to the tunneling regime, with zero-bias maxima instead of minima. The contact resistance R_N up to which well pronounced superconducting anomalies could be seen was the higher the larger the superconducting gap was.

The gap structure at $U = 2\Delta/e$ and its subharmonics due to multiple Andreev reflection agreed well with the BCS value $2\Delta_{\text{BCS}} = 3.52 k_B T_c = 1.05 \text{ meV}$, $352 \mu\text{eV}$, and $165 \mu\text{eV}$ of In, Al, and Cd, respectively (Fig. 11). Strong-coupling Pb had the width enhanced by about 25 per cent with respect to $2\Delta_{\text{BCS}} = 2.20 \text{ meV}$ (Fig. 11). Why the Pb junctions did not have the right energy gap at small resistances we do not know yet. Heating effects or the suppression of superconductivity by the self-magnetic field can be excluded because the other superconductors behave regularly (at

least for junctions with $R_N \geq 10 \Omega$). Some of the Al junctions had lower T_c down to 0.85 K, while some of the Cd junctions had higher T_c up to 0.65 K. This is probably due to disorder and stress in the contact region and resulted in smaller or larger gaps, respectively.

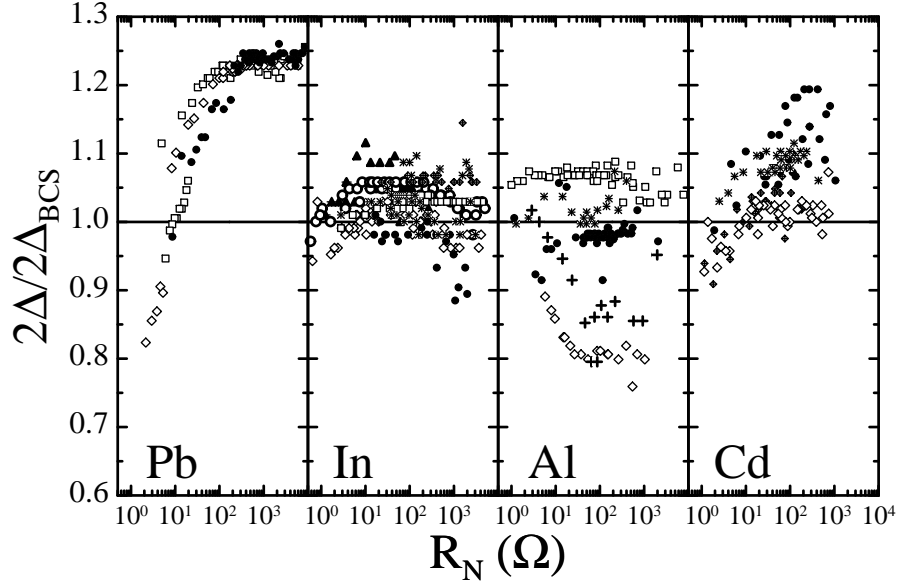


FIG. 11. Experimental superconducting gap 2Δ at $T = 50$ mK vs. R_N , normalized to the BCS value $2\Delta_{\text{BCS}} = 3.52 k_B T_c$. Identical symbols are used in Figs. 11 - 20 for the same pieces of sample.

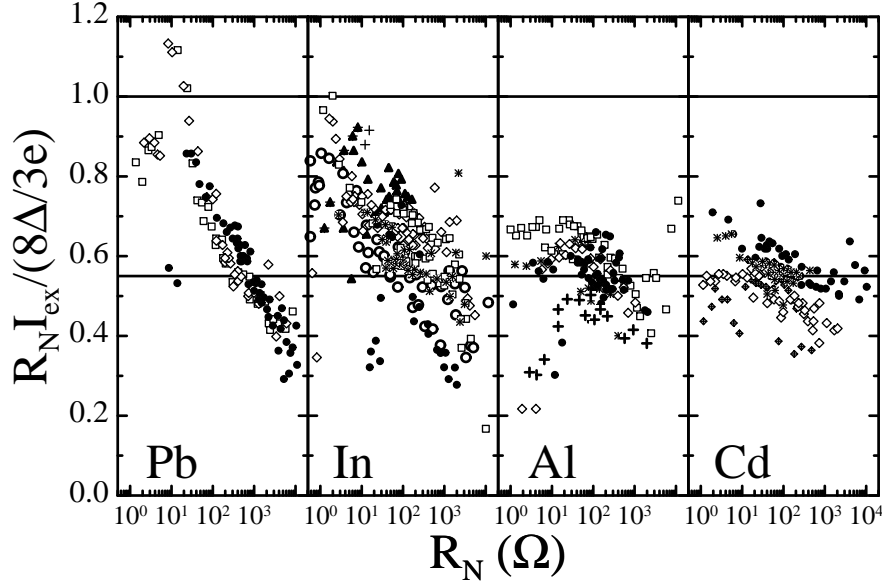


FIG. 12. Experimental $R_N I_{\text{ex}}$ vs. R_N at $T = 50$ mK, normalized to the clean-limit (KO2) value $8\Delta/3e = 3.67, 1.40, 0.47$, and 0.22 mV for Pb, In, Al, and Cd, respectively. Solid lines indicate the KO2 ($= 1.0$) and KO1 ($= 0.55$) value.

A. Andreev-reflection excess current

At small $R_N \approx 1 \Omega$, the excess current I_{ex} was near the clean (KO2) limit for Pb (using the experimental $2\Delta = 2.75$ meV) and In, and near the dirty (KO1) limit for Al and Cd (Fig. 12). This trend could be consistent with the superconducting coherence length $\xi \propto 1/\Delta$ being shorter for Pb and In than for Al and Cd. However, according to the above bulk resistivity data all four superconductors should have been in the clean limit.

At larger R_N and towards the metallic-tunneling transition at $R_K/2$, the excess current of the Pb and In junctions decreased but remained finite, settling around the dirty limit. This reduction may have several reasons: First, small contacts could be stronger distorted than large ones. Second, the junctions could have a finite quasi-particle density of states due to lifetime effects. Using the modified BTK theory³⁰, a reduction of the excess current by a factor two requires a lifetime parameter not larger than $\Gamma = \hbar/\tau \approx \Delta/5$. It agrees roughly with $\Gamma \approx 50 \mu\text{eV}$, estimated using the bulk residual resistivity of the samples. This estimate would be supported by the clearly resolved multiple Andreev reflection anomalies of Pb and In, while Al and Cd show more washed out and smeared structures. Third, normal quasi-particle reflection. Since multiple Andreev reflection is observed, the transmission coefficient D has to be at least somewhat less than 1. An excess current of (on the average) not less than half the maximum possible one, makes the lower bound of the transmission coefficient $D \geq 0.5$. On the other hand, all four superconductors show the transition from vacuum tunneling to metallic conduction at around $R_K/2$, indicating $D \approx 1$.

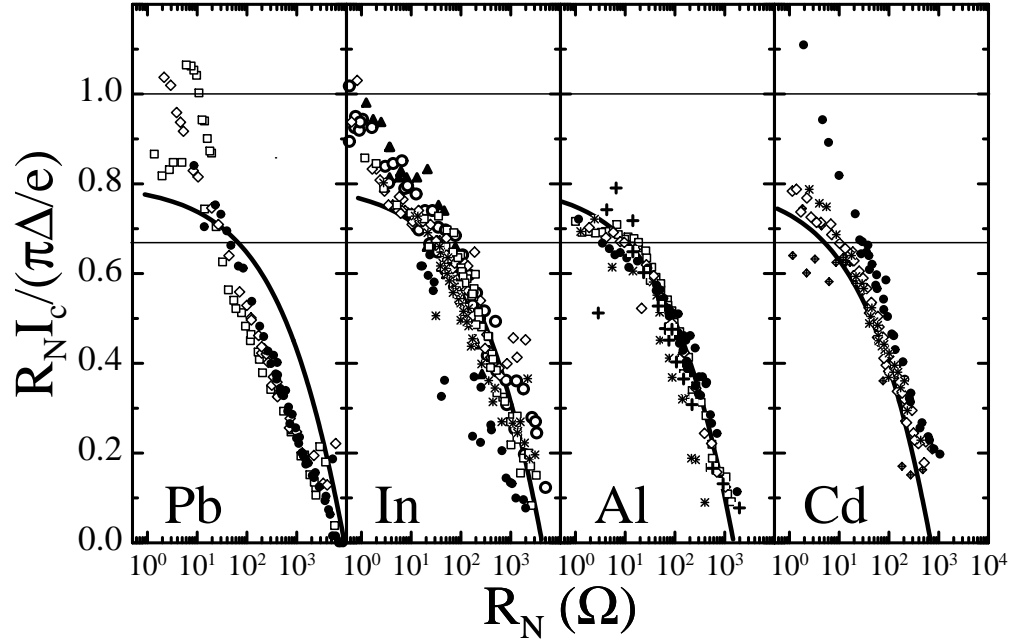


FIG. 13. Experimental $R_N I_c$ vs. R_N at $T = 50 \text{ mK}$, normalized to the clean-limit (KO2) value $\pi\Delta/e = 4.32, 1.65, 0.55$, and 0.26 mV for Pb, In, Al, and Cd, respectively. Solid lines indicate the KO2 ($= 1.0$) and the KO1 ($= 0.66$) result as well as that due to the zero-point fluctuations (Eq. 14) at $C = 0.05 \text{ fF}$ and the abscissa fixed at 0.8 , the best fit for aluminum.

B. Critical current

At small $R_N \approx 1 \Omega$, the critical current I_c (Fig. 13) was near the clean (KO2) limit for Pb and In, and near the dirty (KO1) limit for Al and Cd, like the excess current. But $R_N I_c$ decreased continuously at larger contact resistances and vanished well below $R_K/2$. This agrees with previous observations by others⁵⁻⁸.

Like for the excess current, we would have expected the critical current or the product $R_N I_c$ to be reduced, but to the dirty limit only. Assuming a minimum $D \approx 0.5$ for normal reflection from the Andreev-reflection excess current and applying the current-phase relationship of Eq. 2, the critical current can be reduced by almost a factor two near the Ambegaokar-Baratoff value $\pi\Delta/2eR_N$. Thus the reduction of $R_N I_c$ to zero requires an explanation that does neither affect the superconducting gap nor the excess current. The RCSJ model could solve this problem: the high-resistance part of $R_N I_c$ can be described by Eq. 14 and a small capacitance of $C \approx 0.05 \text{ fF}$. The fit is nearly perfect for Al, but deviates for the other superconductors. Especially the nearly straight line of Pb in the semi-log plot astonishes. These deviations from the theoretical curve at constant C require additional processes, for example a variation of the intrinsic $R_N I_c^0$ at the junction, a varying amount dissipation, or a varying capacitance.

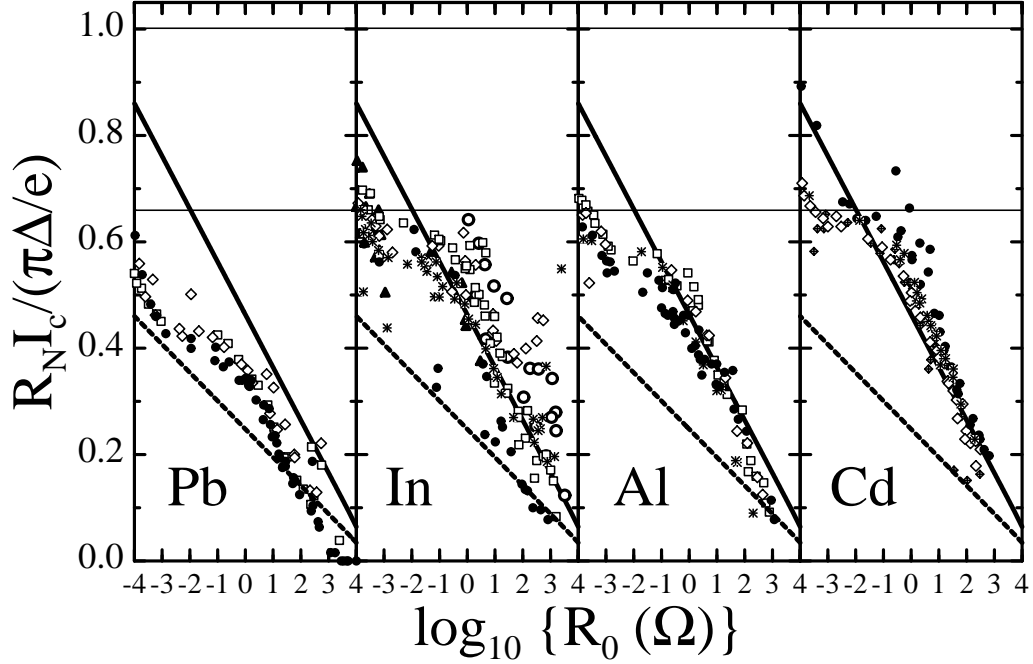


FIG. 14. Experimental $R_N I_c$ vs. R_0 at $T = 50$ mK, normalized to the clean-limit (KO2) value $\pi\Delta/e$. Indicated are the KO2 ($= 1.0$) and the KO1 ($= 0.66$) result as well as that due to phase diffusion Eqs. 26 and 41 at a lead capacitance of $\kappa = 3.3$ pF/m and a quality factor $Q \gg 1$ (solid lines) and $Q = 1$ (dashed lines).

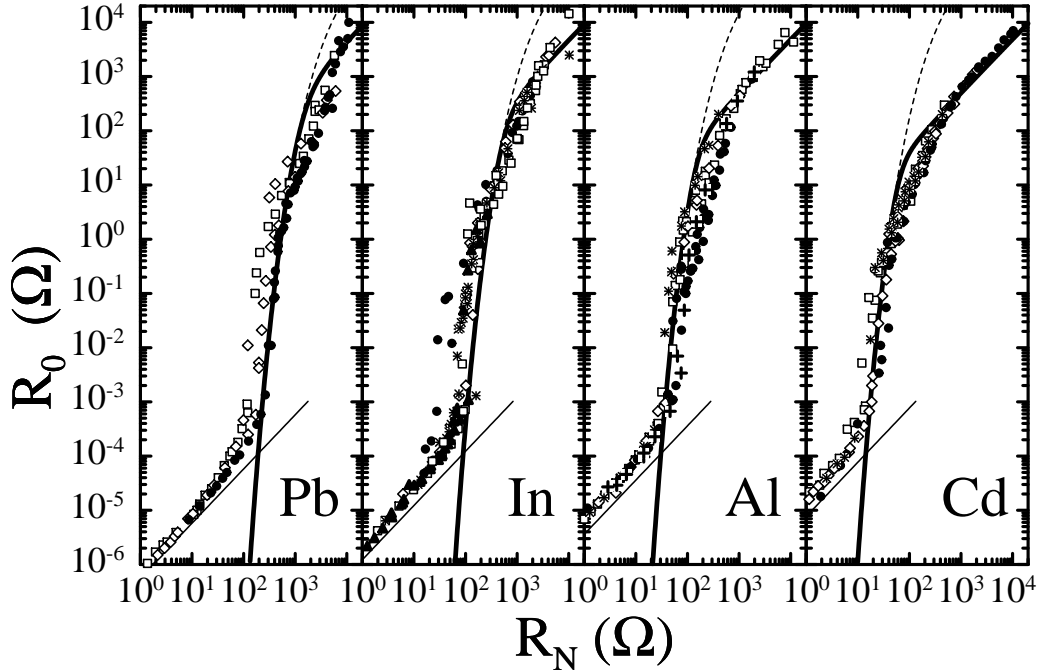


FIG. 15. Residual resistance R_0 vs. R_N at $T = 50$ mK. Straight lines indicate the detection limit, dashed lines are R_0 of Eq. 23 at weak damping $Q \gg 1$, using the clean-limit I_c^0 and $C = 0.05$ fF. Solid lines take into account $R_N/2$ in parallel.

Fig. 14 shows an alternative plot of $R_N I_c$ vs. residual resistance R_0 . Again a systematic decrease is observed when R_0 increases. But this time, all four superconductors behave similarly. The fit through the data points takes into account the dynamic capacitance of the junctions as discussed later.

C. Residual contact resistance

At low R_N the residual contact resistance $R_0 = dU/dI(I = 0)$ was unresolvably small. Here the experimental resolution results from the ~ 2 nV detection limit at a maximum current of I_c . Towards larger R_N the residual resistance emerged out of the detection limit of ~ 2 nV/ I_c , first rising steeply, and then approaching $\sim R_N/2$ (Fig. 15). Again, this behaviour agrees qualitatively with previous observations by others⁵⁻⁸.

Raising the temperature, for example to $T = 2$ K for indium, did barely alter the results. This indicates that the junctions are not thermally activated but are in the regime of quantum tunneling. Only near T_c , when the intrinsic ($R_N I_c^0$) decreases strongly, we also found the transition to a finite R_0 at smaller R_N (Fig. 16).

The data in Fig. 15, especially the steep rise of $R_0(R_N)$, can well be described by Eq. 23 using a constant $C \approx 0.05$ fF as for the critical current in the previous section, the clean-limit I_c^0 , and weak damping. Deviations at large R_N have to be expected: first, the above analysis does not apply when the experimental $R_N I_c = 0$. Second, in the dissipative state the total resistance of the junction can not exceed R_N . It must be less than $R_N/2$ if one includes Andreev reflection, that has not been considered by Eq. 20. Combining phenomenologically these two different regimes, that is R_0 of Eq. 23 and $R_N/2$, by substituting $1/R_0 \rightarrow 1/R_0 + 2/R_N$, fits the data of all four superconductors.

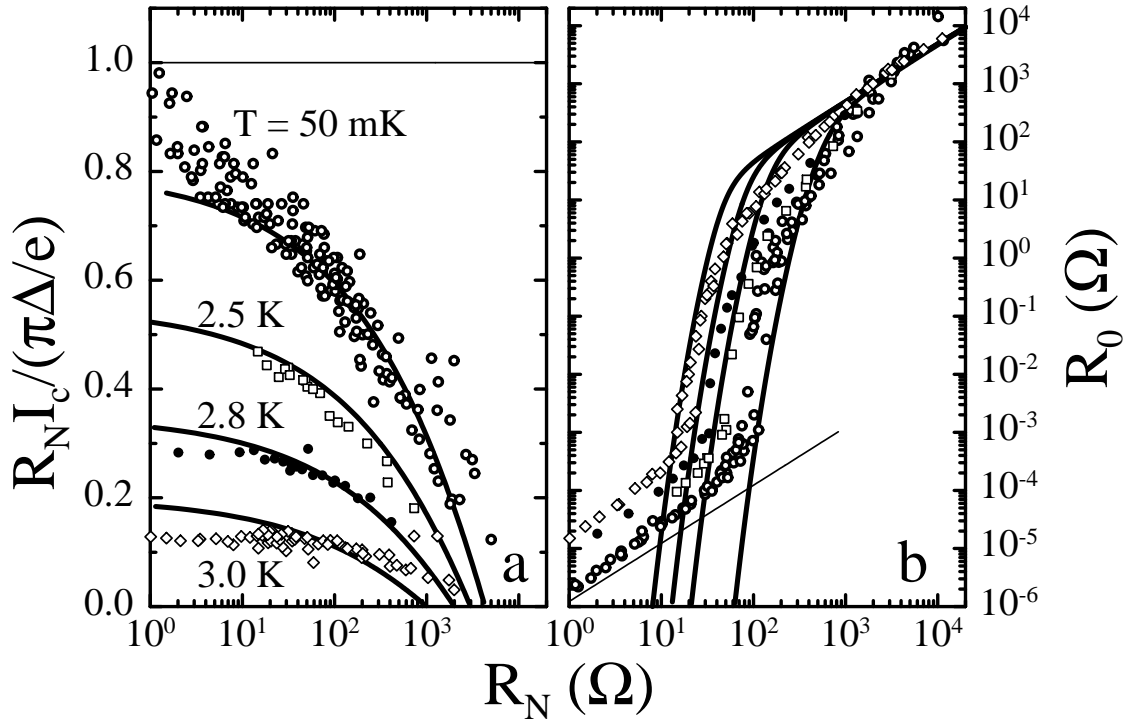


FIG. 16. a) Experimental $R_N I_c$ vs. R_N of In at the indicated temperatures. The data are normalized to the clean-limit (KO2) value $\pi\Delta/e$ at $T \rightarrow 0$. Solid lines result from the zero-point fluctuations Eq. 14 at $C = 0.05$ fF. b) Residual resistance R_0 vs. R_N . Temperatures and symbols as in a). The straight line represents the detection limit for the $T = 50$ mK data, solid lines are R_0 of Eq. 23 using the clean-limit $I_c^0(T)$ and $C = 0.05$ fF, and taking into account the asymptotic $R_N/2$.

D. Plasma frequency and Josephson coupling energy

According to Eqs. 22 - 24 the plasma frequency as well as the coupling energy of each contact with a sufficiently large residual resistance can be derived from the differential resistance at small currents. We find indeed a linear dependence between dU/dI and I^2 (Fig. 17). Its slope divided by R_0 yields directly the plasma frequency ω_p , assuming weak damping $Q \gg 1$. This in turn is used to extract E_{JE} from R_0 . The contacts that can be analyzed this way have residual resistances of ~ 0.1 Ω to ~ 1 k Ω , and according to Fig. 6 their $E_{JE}/\hbar\omega_p$ varies from about 1.2 to 0.5.

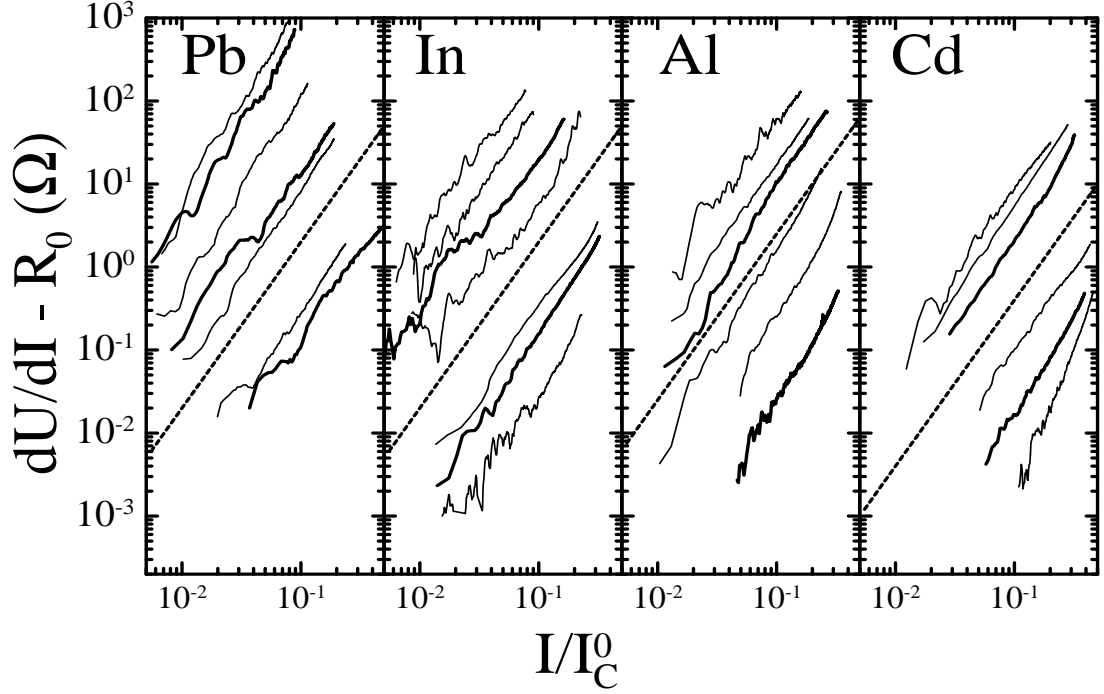


FIG. 17. Typical $dU/dI - R_0$ vs. I/I_c^0 at $T = 50$ mK. Here I_c^0 is the clean-limit value derived from R_N . The dashed lines have a slope of 2 in the double-log plot.

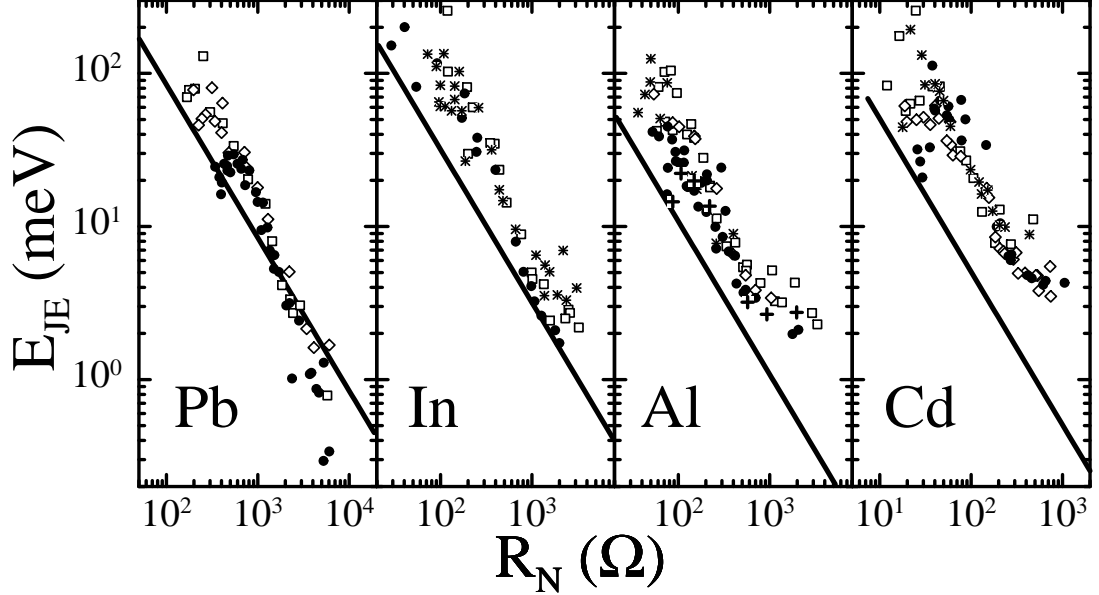


FIG. 18. Josephson coupling energy E_{JE} vs. R_N derived from dU/dI at $I \rightarrow 0$ and at $T = 50$ mK, assuming weak damping $Q \gg 1$. Solid lines are $E_{JE} = \Delta R_K/4R_N$ in the clean limit.

In contrast to the strong reduction of the experimental I_c in Fig. 13, the coupling energy E_{JE} at $I \rightarrow 0$ in Fig. 18 is slightly larger than expected from the clean-limit I_c^0 . The plasma frequency ω_p corresponds to a capacitance of order $C = 0.05$ fF only at large contact resistances (Fig. 19). Deviations at small R_N can not be explained by a reduced escape rate due to stronger damping, because including damping would lead to an even larger ω_p and not to a smaller one. Thus we are forced to conclude that the capacitance C is not a constant. The effective capacitance of the junctions

$$C \approx \frac{4e^2 E_{JE}}{\hbar^2 \omega_p^2} \quad (27)$$

becomes $C \approx 0.1 \text{ fF}/I_c^0 (\mu\text{A})$, depending on the intrinsic critical current (Fig. 20). C does not depend on the geometrical cross sectional area of the junctions which is inversely proportional to R_N . We will show below that it is the above relationship with I_c^0 that has indeed to be expected.

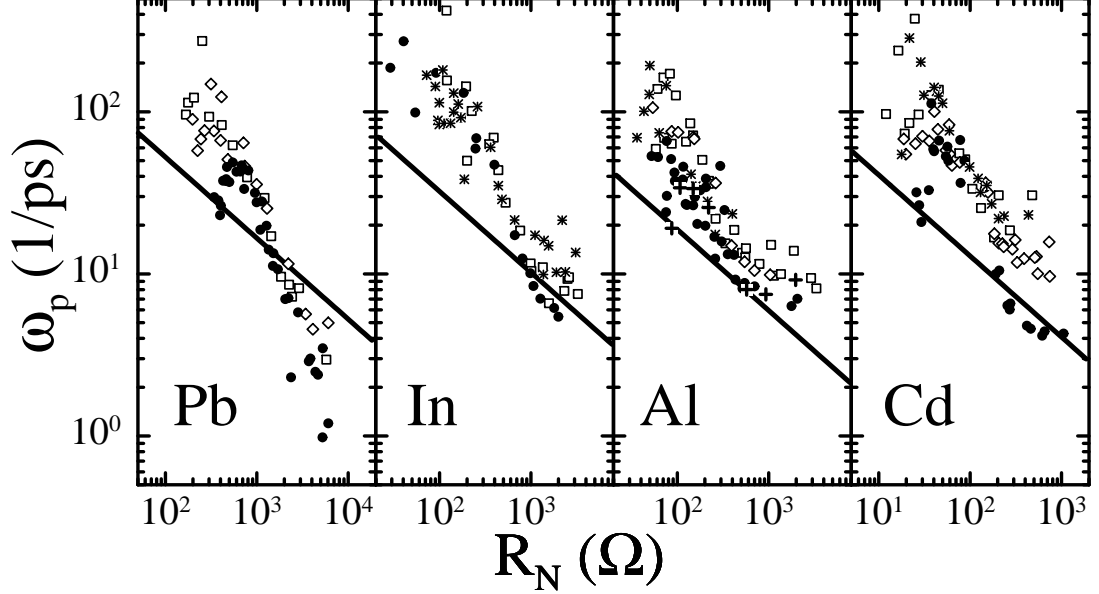


FIG. 19. Plasma frequency ω_p vs. R_N derived from $I(U)$ at $I \rightarrow 0$ and at $T = 50 \text{ mK}$. Solid lines are $\omega_p = \sqrt{2\pi\Delta/\hbar R_N C}$ at $C = 0.05 \text{ fF}$ and in the clean limit.

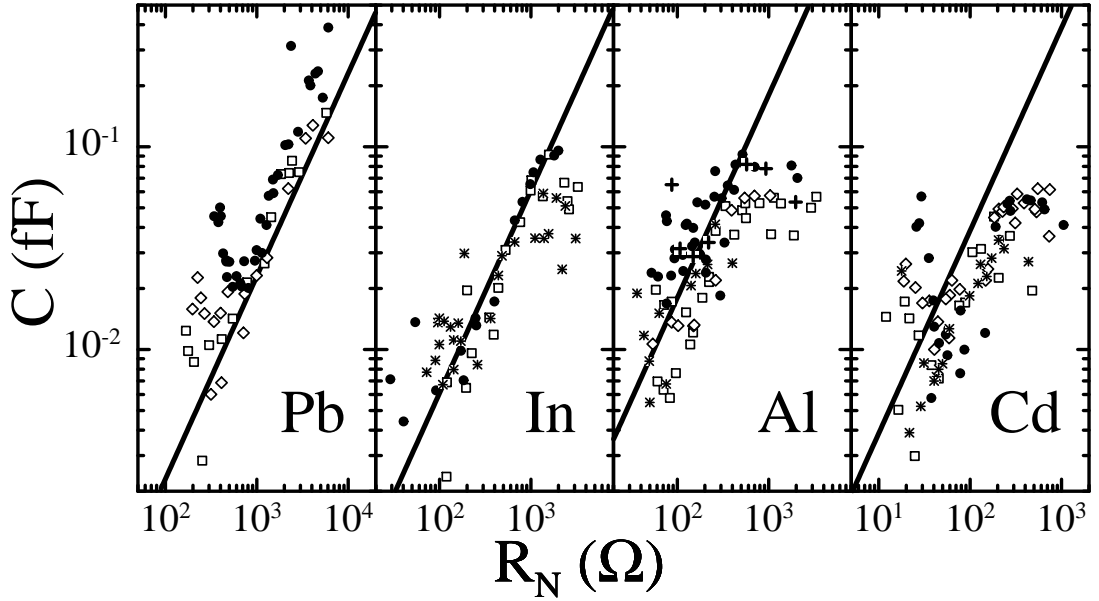


FIG. 20. Capacitance of the junctions C derived from Eq. 27 and the data of Figs. 18 and 19 vs. R_N . Solid lines represent $C = 0.1 \text{ fF}/I_c^0 (\mu\text{A})$ and the clean-limit I_c^0 .

For the junctions with finite R_0 , the $E_{JE}/\hbar\omega_p$ -ratio is always close to one, that is these junctions are very susceptible to quantum fluctuations and phase diffusion. And it requires only slight variations of this ratio to produce the steep

rise of $R_0(R_N)$ because of the large prefactor 14.4 in the exponential function of Eq. 23.

If one assumes $R_{qp} = R_N$, the damping factors $Q = 8\pi R_{qp} E_{JE} / R_K \hbar \omega_p \approx R_{qp} (k\Omega)$ may justify our data analysis using the $Q \gg 1$ limit for the tunneling rate Γ_{QT} and neglecting damping for Pb junctions at $R_N > 1 k\Omega$ but not for Cd, despite both superconductors show similar results. The question arises whether it is correct to describe the damping term of these ballistic junctions by their normal-state resistance R_N . Our experiments seem to indicate that the true quasi-particle resistance of these ballistic Josephson junctions at $I \ll I_c^0$ is much larger than R_N . Such an enhanced R_{qp} has to be expected according to Eq. 5, it finds its natural explanation in the gap of the quasi-particle density of states, that is there are no quasi-particles at all (the clearly resolved multiple Andreev-reflection signal shows that lifetime effects are negligible). Damping can then only be due to losses of the high-frequency electromagnetic field around the junction in the sample and in the metallic part of the setup.

Simultaneously, the absence of hysteretic $I(U)$ -characteristics that would be typical for weakly damped junctions can be explained by strong phase diffusion or drift at I_c that hinders trapping of the phase. One may also speculate whether the Q factor near I_c is smaller than that at $I \rightarrow 0$, due to the frequency dependence of the electromagnetic field generated by the alternating Josephson supercurrent.

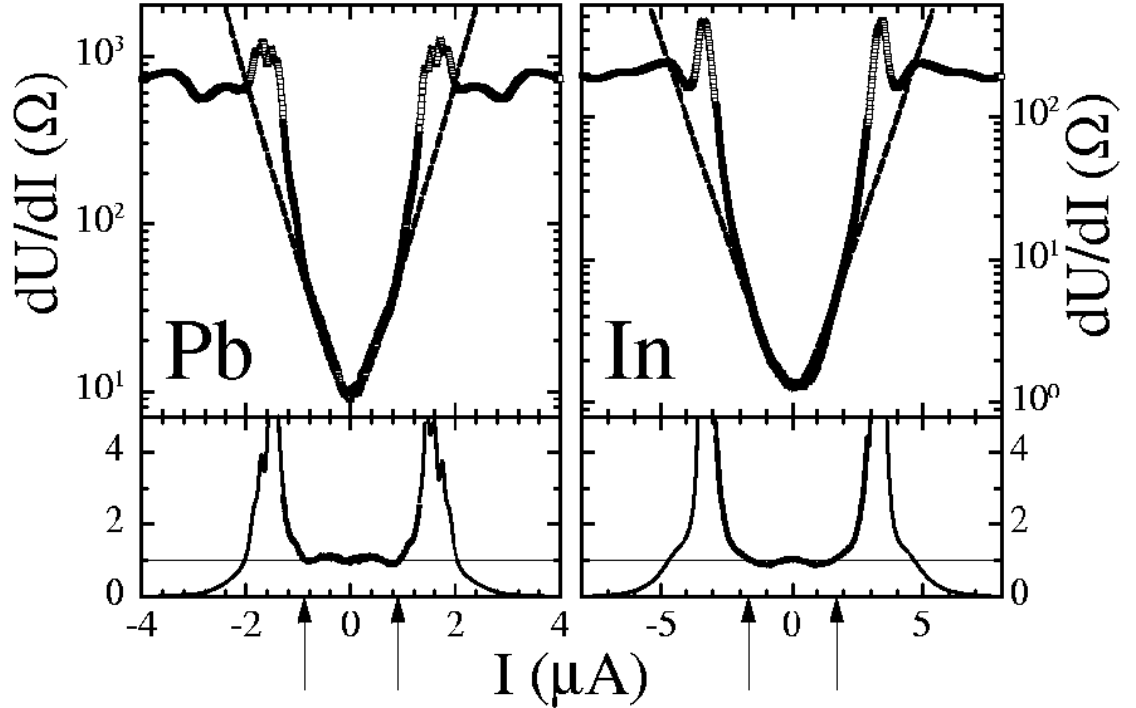


FIG. 21. dU/dI vs. I at $T = 50$ mK of a Pb and an In junction. The dashed lines are fits using Eq. 22. The lower two diagrams show the experimental data normalized to the fit. Arrows mark the current I^* below I_c at which the measured curves starts to deviate from the fit.

E. Zener tunneling of the phase

E_{JE} and ω_p have been derived from the spectra at rather small currents. The intermediate range below the experimental I_c usually shows a steep rise of dU/dI . Some of the junctions, especially those with Pb and In, even have a distinct kink at $I^* \approx 0.2 I_c^0$ (Fig. 21). Such a steep rise has to be expected, and it is straightforwardly explained as Zener tunneling of the phase at $I^* = I_Z$, when the lowest energy level of one of the potential wells exceeds the next higher level of the neighbouring well. This is the more important since $E_{JE} \approx \hbar \omega_p$ of these junctions implies that the washboard potential contains not more than two or three discrete levels. Fig. 22 shows that the agreement between I^* and I_Z is quite good for large ω_p (and small R_0). At small frequencies (and large R_0), the current I^* falls below $e\omega_p/\pi$. This has to be expected, too, because the level spacing of the anharmonic washboard potential decreases when $E_{JE}/\hbar\omega_p$ decreases.

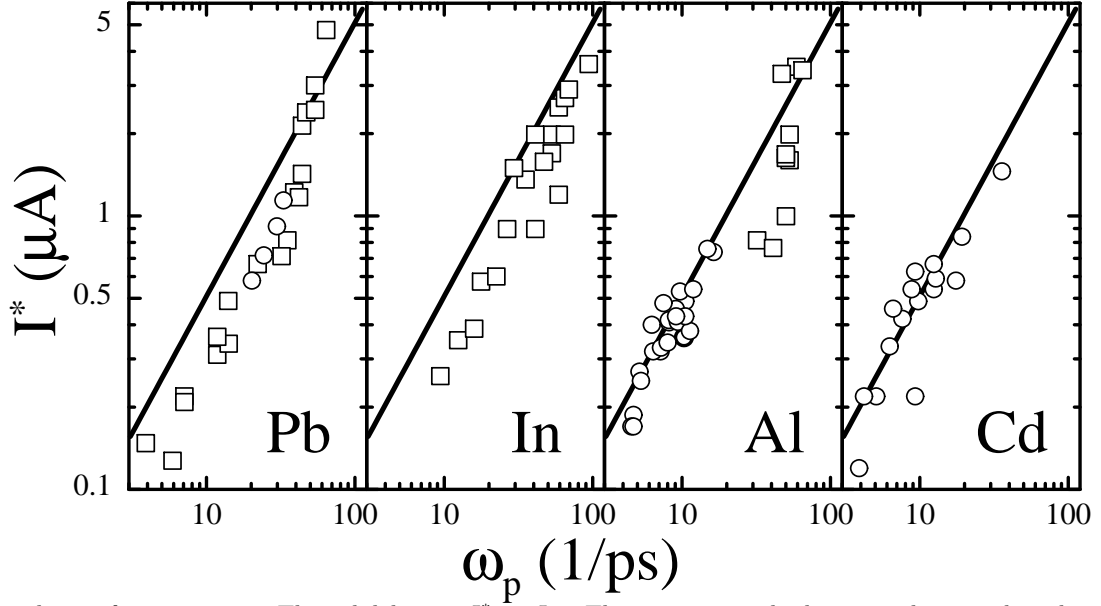


FIG. 22. I^* vs. plasma frequency ω_p . The solid line is $I^* = I_Z$. The squares mark the anomalies attributed to Zener tunneling of the phase, circles denote the position of the minima of the spectra.

Nevertheless, Zener tunneling of the phase implies that the junctions are only weakly damped. Otherwise, the experimental R_0 would yield $E_{JE}/\hbar\omega_p \leq 0.5$, and the washboard potential would have not more than one discrete level. As Zener tunneling features could be observed at junctions with R_0 up to about 260, 175, and $15\ \Omega$ for Pb, In, and Al, respectively, the quality factor $Q \geq 5$. This supports our interpretation in the previous section.

Zener tunneling of the phase is preferably resolved at Pb or In junctions and not at Al or Cd junctions. The simplest explanation is that the voltage drop at $I = I_Z$

$$U_Z \approx \frac{\sinh(3.6)}{3.6\pi} e\omega_p R_0 \quad (28)$$

of about $0.26\ \mu\text{V} \cdot \omega_p(1/\text{ps})R_0(\Omega)$ has to be considerably smaller than the superconducting gap $2\Delta/e$. This condition is the easier fulfilled the larger the energy gap is, that is for Pb and not for Cd.

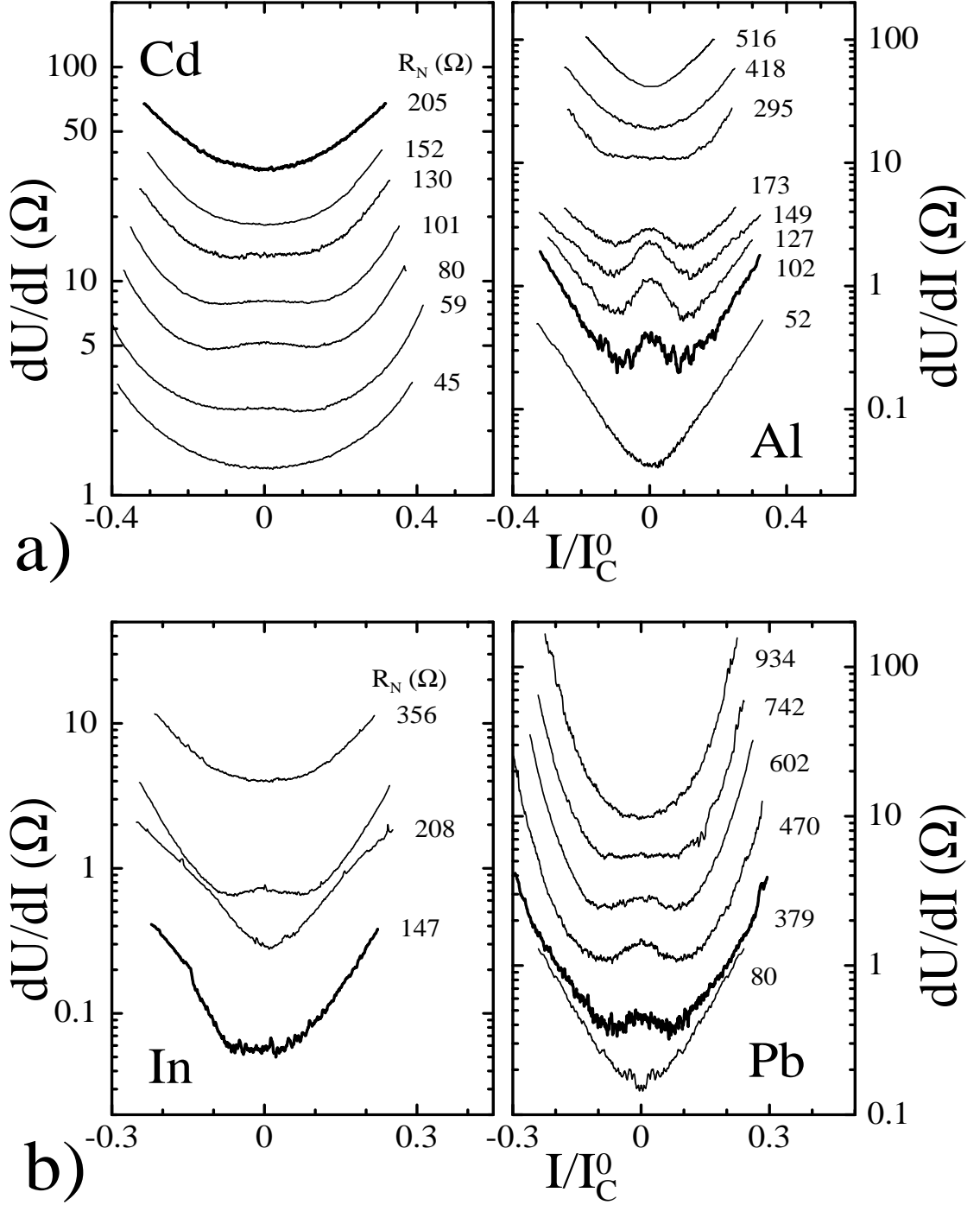


FIG. 23. dU/dI vs. I/I_c^0 at $T = 50$ mK of some selected junctions showing additional double-minimum structures around $I^* = 0.1 I_c^0$. I_c^0 with the clean-limit critical current.

F. Possible excitation of Bloch waves

One source of uncertainty in deriving both E_{JE} and ω_p are additional structures – zero-bias maxima – superposed on $dU(I)/dI$ of some of the junctions (Fig. 23). They were observed quite often for Al and Cd and less often for Pb and In. Conventional explanations for such zero-bias maxima are Kondo scattering at magnetic impurities or Andreev reflection at a normal-superconducting interface. Both explanations seem to be feasible here, because they only require a small normal interfacial region or a tiny amount of Kondo impurities (on the ppm level), that may have

been introduced by cutting the nut. But these two phenomena should take place at nearly constant voltage, while the experimental data are clearly related with a current of $I^*/I_c^0 \approx 0.1$.

An alternative explanation is Coulomb blockade with its negative contribution to dU/dI , and one may speculate whether these additional anomalies in Fig. 23 result from the excitation of Bloch waves, like in Ref.²⁷. In favour of this interpretation is that in the previous paragraph we have found hints that the damping is smaller than expected and the quasi-particle resistance much larger than R_N . However, our junctions have Coulomb charging energies $E_C = (\hbar\omega_p)^2/8E_{JE} \approx E_{JE}/10$, that means they are in the tight-binding limit. If there was a Coulomb blockade then it can not be expected to be well pronounced, like what is seen in Fig. 23. The transport of Cooper pairs could also be enhanced when the periodic transfer of Cooper pairs is in resonance with the zero-point oscillations of the Josephson plasma. The position I^* of the minima marks then the Zener current I_Z for tunneling of the quasi-charge. As a cross-check, we estimate E_{JE} from R_N by assuming the theoretical I_c^0 and calculate then ω_p from the experimental R_0 . Indeed, the position I^* of the minima fits reasonably well the above estimated plasma frequency, that is $\pi I^*/e \approx \omega_p$, see Fig. 22.

A negative contribution could be superposed on the dU/dI spectra of the other junctions, even if a minimum cannot be resolved. The relative size of such a contribution may depend on damping, that is on the (unknown) quasi-particle resistance R_{qp} . The plasma frequency and, consequently, the coupling energy would then have been overestimated. However, in view of the available experimental data, these possible corrections are difficult to handle.

G. Noise

Up to now we have neglected electrical noise. Since noise can also drive the junctions towards the resistive state, we have to ensure that it is small enough. A natural measure for the noise magnitude is the superconducting gap 2Δ . Low-frequency noise up to about 2 MHz makes no problem, we can detect it directly: including amplifier noise, it is less than about $2 \mu\text{eV}$ ($10 \mu\text{eV}$) at a 100Ω ($10 \text{k}\Omega$) resistor and comparable to the thermal noise $k_B T \approx 4 \mu\text{eV}$ at our lowest temperature of 50 mK. This is much smaller than 2Δ of the four superconductors, and it is consistent with the fine structure of the spectra due to multiple Andreev reflection in Fig. 10.

The possible radio-frequency component of the external noise, however, can only be revealed indirectly through the properties of the junctions. For this reason we can not *prove* that this sort of noise is negligible. Let us assume, for the moment, that the finite R_0 as well as the reduced I_c mainly result from external noise. What is then the minimum noise level required to explain these results? Weakly damped junctions in the thermally activated regime are used for this estimate because including damping and assuming quantum tunnelling would require more noise. The tunneling rate is then given by the well-known Arrhenius law

$$\Gamma_{TA} = \frac{\omega_p}{2\pi} \exp\left(-\frac{2E_{JE}}{k_B T_{\text{eff}}}\right) \quad (29)$$

T_{eff} is an effective temperature $T_{\text{eff}} = T + T_{\text{noise}}$, that is we assume white noise with an equivalent temperature T_{noise} , and superpose it on the thermal noise of the junctions. Using the same arguments as for quantum tunneling Eqs. 20-24, the differential resistance at $I \rightarrow 0$

$$dU(I)/dI \approx R_0 \cosh\left(\frac{\pi\hbar}{2ek_B T_{\text{eff}}} I\right) \quad (30)$$

Here the residual resistance $R_0 = dU/dI(I=0)$

$$R_0 \approx R_K \frac{\hbar\omega_p}{4k_B T_{\text{eff}}} \exp\left(-\frac{2E_{JE}}{k_B T_{\text{eff}}}\right) \quad (31)$$

The second-order approximation of Eq. 30

$$\frac{dU(I)}{R_0 dI} \approx 1 + \frac{1}{2} \left(\frac{\pi\hbar I}{2ek_B T_{\text{eff}}}\right)^2 \quad (32)$$

now allows to derive the effective temperature of the junctions from the spectra at $I \rightarrow 0$. By comparing the I^2 -dependence of Eq. 32 with that of Eq. 24, we can directly read off

$$k_B T_{\text{eff}} = \hbar\omega_p/3.6 \quad (33)$$

from the data in Fig. 19 (the ω_p in Eqs. 29 and 33 denote different parameters). This yields *lower* bounds for the hypothetical noise temperature in the 1 - 100 K range. If such a noise level was real, we would never have seen any superconducting features of our samples. Thus we conclude that the external noise level is much smaller than the zero-point energy of the junctions, and ω_p in Fig. 19 is the plasma frequency.

The shape of the $I(U)$ -characteristics at I_c responds more sensitively to external noise than the residual resistance. The pronounced kink at the critical current of an ideal $I(U)$ -characteristic can be rounded, and both the hysteresis and I_c can be reduced when the noise level exceeds even a small fraction of the coupling energy E_{JE} , see for example Ref.²¹. To observe this noise, its size must be at least comparable to the zero-point energy of the particle in the tilted washboard potential. Since increasing the current means to reduce the minimum height of the potential wells $2E$ as well as the zero-point energy $\hbar\omega/2$, at some current below the intrinsic critical one, thermal or external noise should definitely overtake. However, in contrast to the analytical Eq. 11, the zero-point energy has a lower bound as described by Eqs. 12 and 13. This is due to the fact that the flow of supercurrent needs at least one discrete energy level. Those junctions with finite R_0 , for which we can derive the plasma frequency, would require noise temperatures in the 1 - 1000 K range. Such a noise level is by far too large, as found above while discussing the possible effects of noise on R_0 and the $I(U)$ -characteristic at $I \rightarrow 0$. Towards smaller contact resistances, the experimental $E_{JE}/\hbar\omega_p$ ratio increases slightly, the critical current approaches the theoretical I_c^0 (at least for Pb and In), and the minimum ω can be much smaller than ω_p . But the absolute value of ω_p also rises if we extrapolate the data in Fig. 19, so the necessary noise level will not go down. The hysteresis found at some of the low-resistance junctions in the $R_N = 1 - 10 \Omega$ range could be explained by low damping, although heating effects can not be excluded. At larger contact resistances, the minimum required noise level becomes smaller than about $T_{\text{noise}} \approx 1$ K. It is then quite possible that external noise contributes to the spectra. We conclude that the rounding of the $I(U)$ -characteristics as well as the reduction of I_c mainly originates from the quantum-mechanical zero-point fluctuations as an *internal* noise source of our Josephson junctions and not from external noise. Of course, it is this internal noise that can also strongly reduce the hysteresis of the $I(U)$ -characteristics.

There are additional arguments that noise can indeed be neglected:

- a) Our experimental observations agree qualitatively with previous ones by others who used a similar type of setup for preparing the break junctions⁵⁻⁸. If external noise was the limiting factor, then the noise level should be the same in both experiments. But it is unlikely to have an identical noise level at these various experiments and at different times and locations.
- b) A different series of break-junction experiments on doped semiconductors (Germanium) using our setup indicated a noise level of less than about $50 \mu\text{V}$ for junctions with $R_N < 100 \text{ k}\Omega$, and corresponding to a noise temperature of less than about 0.5 K. Thus the total noise at the junctions consist mainly of the low-frequency component.
- c) If the high-frequency noise would dominate, it would roughly be related to the experimental zero-point energy $\hbar\omega_p/2$, as discussed above. We expect junctions with larger R_N to pick up more noise than those with smaller R_N , independent of the superconducting gap. Quite contrary, the experimental ω_p in Fig. 19 *decreases* almost like Δ/R_N . Note that for these junctions $\hbar\omega_p/2 \geq 2\Delta$.
- d) Both the experimental critical current I_c from $I(U)$ at large currents and the $I(U)$ characteristic at $I \rightarrow 0$ consistently indicate a small capacitance of order 0.1 fF.
- e) The experimental E_{JE} derived from $dU(I)/dI$ at $I \rightarrow 0$ nearly coincides with the theoretical coupling energy (Fig. 18). There is no adjustable parameter.
- f) Although rather different processes (Zener tunneling of the phase as well as the excitation of Bloch waves and Zener tunneling of the quasi-charge) may contribute to the spectra at $I^* \approx I_Z$, this marker closely corresponding to $e\omega_p/\pi$ supports our derivation of the plasma frequency.

We believe these arguments as a whole strongly support the basic concepts of our interpretation. What is needed now is to understand the physical meaning of the capacitance of metallic Josephson junctions.

H. The horizon model of tunnel junctions

Future research on superconductors with even lower T_c , those that have gaps with nodes of zeroes, or gaps with unknown symmetry like the heavy-fermion superconductors, requires to reduce the quantum fluctuations by increasing the capacitance.

It is difficult to extract the capacitance of solitary junctions. This problem has been discussed extensively for the case of Coulomb blockade at tunnel junctions, see for example Refs.³³⁻³⁶, applying Nazarov's horizon model³⁷. Our break junctions in the vacuum-tunneling regime, when the two halves of the sample are not in direct contact but are separated by a 0.1 - 1 nm wide vacuum gap, and in the normal state have an asymptotic offset of their $I(U)$

characteristic at ~ 50 mV in the range 0.2 - 2 mV. Attributing this offset to Coulomb blockade, we estimate an intrinsic capacitance C_0 of order 0.1 fF due to the vacuum gap.

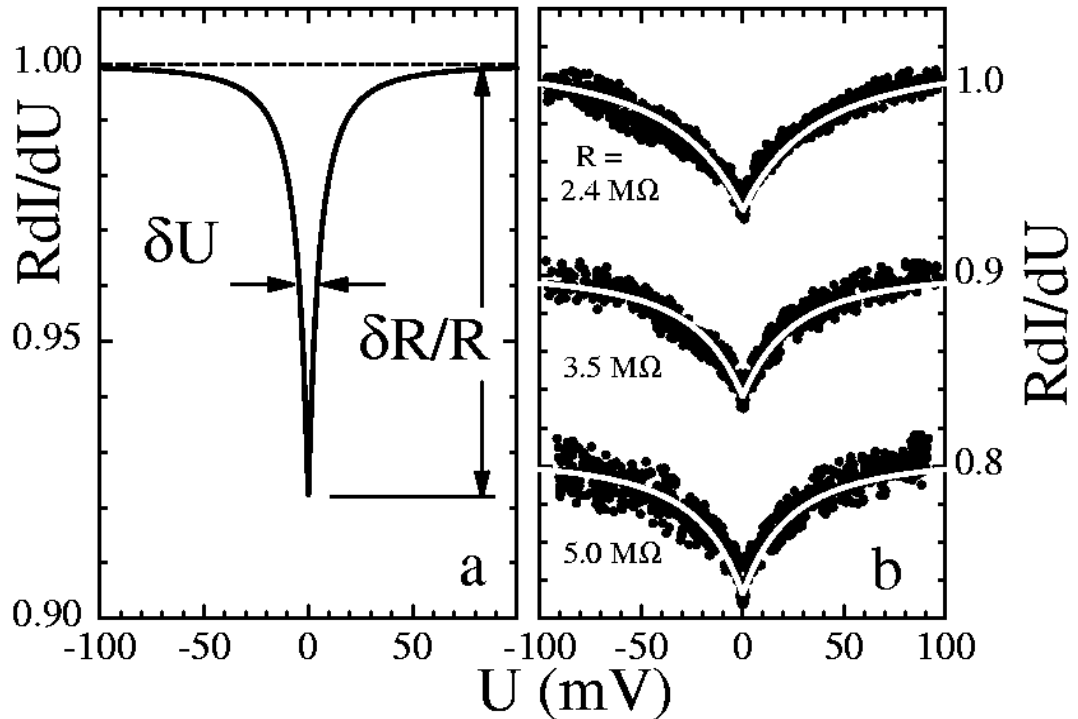


FIG. 24. a) Normalized conductance of a tunnel junction with a constant $1/R = dI/dU$ (dashed line), modified by Coulomb blockade Eq. 36 (solid line). The relative size $\delta R/R$ of the zero-bias anomaly determines the lead capacitance κ , assumed to be $\kappa = 5$ pF/m. The capacitance C_0 , here 0.1 fF, is inversely proportional to both the width δU and $\delta R/R$. b) Experimental data of Al junctions in the normal state at $T = 50$ mK. Superconductivity has been suppressed by a magnetic field of $B = 100$ mT. R is the differential resistance at $U \approx 100$ mV. The two lower spectra have been shifted for clarity. The solid lines are fits using Eq. 36 with $\kappa \approx 5 - 6$ pF/m. The intrinsic capacitance $C_0 \approx 20$ aF.

At smaller voltages the lead capacitance enhances the total capacitance with respect to C_0 . The leads – which means here not only the current and voltage leads but also the two halves of the sample and the close surroundings of the junction itself – can be treated as a transmission line with a capacitance per length κ . The Heisenberg uncertainty principle now defines the shortest time scale for the relevant processes at the junction, and thus a maximum spread or horizon of about³⁷ $\hbar c/e|U|$ (at $U = 1$ mV this spread amounts to about $188 \mu\text{m}$). Here c denotes the speed of light. The total capacitance becomes then

$$C(U) \approx C_0 + \frac{\kappa \hbar c}{e|U|} \quad (34)$$

diverging at $U \rightarrow 0$. To incorporate Coulomb blockade into the low-temperature spectrum of a tunnel junction with constant conductance $1/R = dI(U)/dU$, its $I(U)$ characteristic is displaced by $e/2C(U)$ on the voltage axis, that is

$$RI \approx U - \frac{e}{2C(U)} \text{sign}(U) \quad (35)$$

The normalized conductance becomes

$$R \frac{dI}{dU} \approx 1 - \frac{e^2 \kappa \hbar c}{2(e|U|C_0 + \kappa \hbar c)^2} \quad (36)$$

At large voltages $dI/dU = 1/R$ is recovered, but there is a $\delta R/R = e^2/2\kappa \hbar c$ deep minimum at $U = 0$, see Fig. 24. With this dip the lead capacitance amounts to

$$\kappa \approx \frac{e^2}{2\hbar c} \frac{R}{\delta R} \quad (37)$$

C_0 can then be estimated from the width δU of the anomalies. For our vacuum tunnel junctions (Fig. 36) we get an average $\kappa \approx 5$ pF/m (for the different junctions κ was found to vary between about 2 pF/m and 10 pF/m). This is a quite reasonable value, although being smaller than typical literature data reported for tunnel junctions, for example $\kappa \approx 10$ pF/m³³ and $\kappa \approx 20 - 32$ pF/m³⁵.

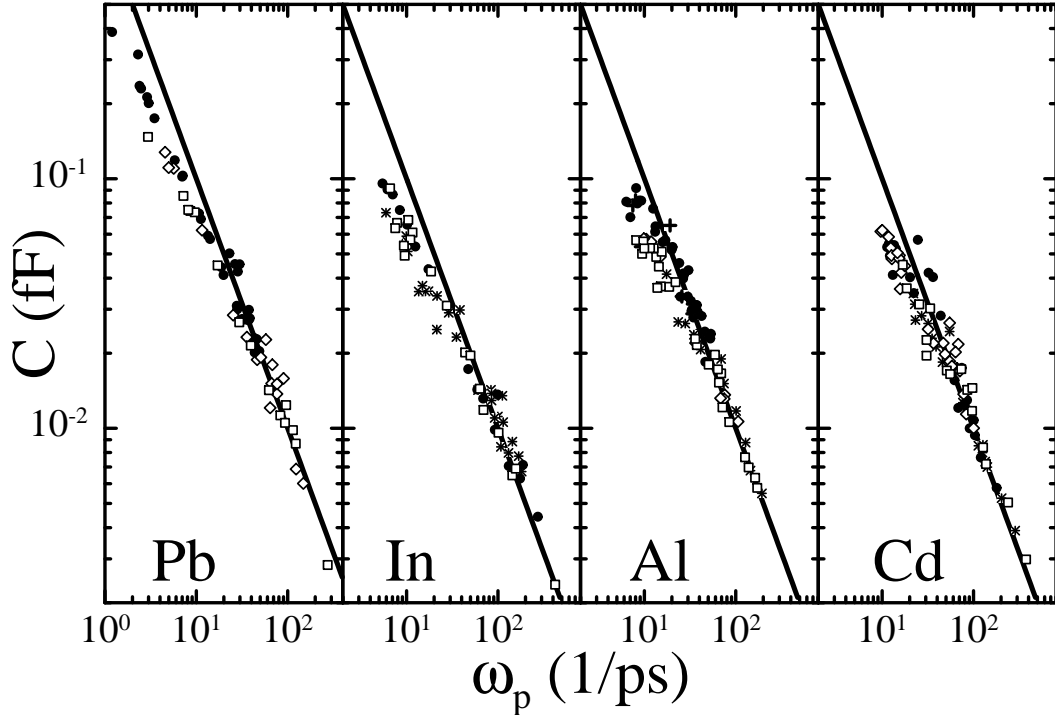


FIG. 25. Capacitance $C = 4e^2 E_{JE} / \hbar^2 \omega_p^2$ vs. plasma frequency ω_p of the Josephson junctions. The solid lines represent $C = \kappa c / \omega_p$ with $\kappa = 3.3$ pF/m.

I. The dynamic capacitance of metallic Josephson junctions

Metallic junctions have an intrinsic $C_0 = 0$, that is only the dynamic capacitance contributes. The small experimental capacitances in Fig. 20 together with the lead capacitance κ estimated in the previous section reveal an horizon of $C/\kappa \approx 1 - 100 \mu\text{m}$, restricted to the immediate vicinity of the junctions. The huge capacitances (~ 0.1 nF) of the external current and voltage leads do not matter, in contrast to the interpretation in Refs.^{7,8}. How to derive theoretically the horizon of a ballistic Josephson junction?

The theory for tunnel junctions^{37,34} is based on the idea that the charge transfer across the junction creates an excess charge on the other lead. This excess charge is transported down the leads via photons with arbitrary low energy. The new state is orthogonal to the equilibrium ground state, yielding an infrared divergency. In the quantum regime of the junction, the divergency manifests itself as a zero-bias anomaly with a power law. We do not know whether such a theory can be applied to metallic Josephson junctions investigated here. However, we will use the physical idea that the infrared divergency, caused by the interaction of the system with its electromagnetic environment, is cut off at the lowest characteristic frequency of the problem.

The RCSJ model maps the many degrees of freedom of the electron system involved in charge transfer across a Josephson junction onto a single degree of freedom, the phase difference φ between the two bulk superconductors. Since phase and charge density are canonically conjugated variables, and the electromagnetic gauge field couples to the charge, its quantum fluctuations modify dynamically the capacitance of the junction. Moreover, the interactions with the electromagnetic field are strong enough to *define* the capacitance (or mass) of the particle in the washboard potential. The ground state of the quantum-mechanical model of a Josephson junction even at finite current $I < I_c$ is a meta-stable one. It can be described by the ground state of an harmonic oscillator with the Josephson plasma frequency ω_p and a zero-point energy $\hbar\omega_p/2$. A constant expectation value $\langle \varphi \rangle$ leads to $U = 0$, although the charge fluctuations of the ground state take place on a time scale $1/\omega_p$. Since this is the only time scale of the system, we

expect ω_p to play the crucial role as cut-off frequency in defining the horizon. And this will yield a self-consistent picture for the interpretation of our experimental results.

A different approach is known in quantum mechanics: a conventional particle of mass m interacting with a relativistic quantum field. This interaction includes a certain environment around the particle, limited by a cut-off parameter $\sim c\hbar/mc^{238}$. This cut-off – which is just the horizon we are looking for – depends on the internal energy mc^2 of the particle. It serves to avoid the creation of additional particles, excluded in the non-relativistic treatment of the particle itself. Applying this model to a Josephson junction lacking a real mass, the internal energy mc^2 has to be replaced by the excitation energy $\hbar\omega_p$ to avoid transitions between the ground state and the next higher level.

Both models thus predict the same horizon $\sim c/\omega_p$. The total capacitance becomes then

$$C \approx \kappa c/\omega_p(C) \quad (38)$$

Note that ω_p is a function of C with a *positive* feedback: the higher the frequency the smaller is the capacitance, further enhancing the plasma frequency. Solving for C and ω_p yields

$$C \approx \frac{\kappa^2 c^2 \hbar}{2eI_c^0} \quad (39)$$

and

$$\omega_p \approx \frac{2eI_c^0}{\kappa c \hbar} \quad (40)$$

respectively. The experimental data in Figs. 19 and 20 reproduce indeed such a dependence from $I_c^0 \propto 1/R_N$. The absolute values of $C(\omega_p)$ of the four investigated superconductors in Fig. 25 fit almost perfectly a $\kappa \approx 3.3$ pF/m. The good agreement with $\kappa \approx 5$ pF/m estimated above for the tunnel junctions, supports our interpretation.

Since frequency and capacitance are related to each other, Eqs. 39 and 40 are valid only at $I \rightarrow 0$, like Eq. 27. When the applied current approaches the intrinsic I_c^0 , the capacitance should become larger because the plasma frequency decreases. Near I_c^0 the capacitance should diverge (this is partly compensated by the applied current introducing an additional time scale or frequency $\sim I/e$). For this reason the relation Eq. 14 can not adequately describe the experimental data (disregard the correct order of magnitude of C), that is quantum fluctuations only indirectly suppress the critical current.

Most of the critical current data in Fig. 13 have been reduced with respect to the theoretical I_c^0 . Therefore it seems reasonable to assume $C(I_c) \approx C(I \rightarrow 0)$. Phase diffusion at $|\dot{\varphi}| \geq \omega_p$ becomes then responsible for I_c being too small. As the Zener current $I_Z = e\omega_p/\pi = 4I_c^0/\kappa c R_K$, the critical current at $Q \gg 1$ amounts to

$$I_c \approx \frac{I_c^0}{0.9\kappa c R_K} \operatorname{arcsinh} \left(\frac{1.8R_K}{R_0} \right) \quad (41)$$

This I_c depends directly on the residual resistance. Eq. 41 fits the experimental data quite well, see Fig. 14. No adjustable parameter is required because the lead capacitance κ is known from the spectra at $I \rightarrow 0$. Considering damping reduces the critical current of Eq. 41 by a factor of about $[1 + 0.87/Q]$. The close coincidence between $R_N I_c(R_0)$ and Eq. 41 thus excludes any strong effect from damping. It supports our above estimate of $Q = \omega_p R_{qp} C = \kappa c R_{qp} \geq 1$, and the quasi-particle resistance of the ballistic junctions being considerably larger than R_N .

There seem to be several possibilities to reduce the lead capacitance κ and drive the junctions towards the delocalized Coulomb blockade limit, or to make it larger and get more localized Josephson-like behaviour. To enlarge the lead capacitance κ by increasing the accessible volume or by bringing the junctions closer to the conducting ground plane than is possible with bulk samples, one should use junctions made of thin films like that described in Ref.³⁹ or whiskers. On the other hand, the conduction electrons around the junction of a bulk sample reduce the effective volume of the capacitor, as long as ω_p is smaller than the plasma frequency $\sim 10^4$ ps⁻¹ of the conduction electron system, as already proposed by K. K. Likharev⁴⁰. In an extreme limit, the Josephson junction is completely embedded in normal metal. Alternating currents and fluctuations could then exist only at frequencies above the plasma frequency of the conduction-electron system, enhancing the quantum fluctuations by driving the effective capacitance towards zero. Such junctions with strongly reduced critical currents may have been realized already with the so-called heavy-fermion superconductors. At junctions with these superconductors a considerable part of the contact region seems to be driven normal due to stress and disorder, and the product $R_N I_c$ was found to be several orders of magnitude smaller than expected, see e. g. Ref.⁴. To take into account a small C may be an interesting new aspect for the future study on those superconductors.

V. SUMMARY

The quantum-mechanical treatment of the RCSJ model explains quite well the properties of superconducting point contacts over a wide range of resistances. The small capacitance of the junctions reproduces both the suppression of the critical current and the finite contact resistance by phase diffusion and drift due to quantum tunneling at the presence of large quantum-mechanical fluctuations of the Josephson plasma. Our interpretation does not require external noise and the huge capacitances of the current and voltage leads. A detailed analysis of the $I(U)$ characteristics and $dU(I)/dI$ spectra reveals a frequency-dependent capacitance of the junctions that is well described by the horizon model, that has first been applied to tunnel junctions. The lead capacitance is the only free parameter with which one can almost fully understand our Josephson junctions. Combining the properties of the metallic Josephson junctions with that of a completely different type of vacuum tunneling junctions in the normal state strongly supports our interpretation. There are several hints that the metallic Josephson junctions possess a rather large quasi-particle resistance $R_{qp} \geq 1 \text{ k}\Omega$. They are therefore only weakly damped, and anomalies which we have attributed tentatively to the excitation of Bloch waves, Zener tunneling of the quasi-charge, and Zener tunneling of the phase become plausible even though the normal-state resistance of the junctions is less than $R_K/4$.

ACKNOWLEDGMENTS

F. A. thanks A. van Otterlo for discussions. This work was supported by the SFB 252 Darmstadt/Frankfurt/Mainz and the German BMBF Grant No. 13 N 6608/1.

-
- ¹ J. M. Martinis, M. H. Devoret, and J. Clarke, Phys. Rev. **B 35**, 4682 (1987)
² J. C. Cuevas, A. Martín-Rodero, and A. Levy Yeyati, Phys. Rev. **54**, 7366 (1996)
³ A. Levy Yeyati, A. Martín-Rodero, and J. C. Cuevas, J. Phys.: Condens. Matter **8**, 449 (1996)
⁴ K. Gloos, F. B. Anders, W. Abmus, B. Buschinger, C. Geibel, J. S. Kim, A. A. Menovsky, R. Müller-Reisener, S. Nuettgens, C. Schank, G. R. Stewart, and Yu. G. Naidyuk, J. Low Temp. Phys. **110**, 873 (1998)
⁵ C. J. Muller, J. M. van Ruitenbeek, and L. J. de Jongh, Physica **C 191**, 485 (1992)
⁶ C. J. Muller, M. C. Koops, B. J. Vleeming, R. de Bruyn Ouboter, and A. N. Omelyanchouk, Physica **C 220**, 258 (1994)
⁷ E. T. Peters, *Ph. D. Thesis*, Leiden (1995), unpubl.
⁸ N. van der Post, *Ph. D. Thesis*, Leiden (1997), unpubl.
⁹ B. D. Josephson, Phys. Lett. **1**, 251 (1962)
¹⁰ V. Ambegaokar and A. Baratoff, Phys. Rev. Lett. **10**, 486 (1963); Phys. Rev. Lett. **11**, 104 (1963);
¹¹ I. O. Kulik, A. N. Omel'yanchuk, JETP Lett. **21**, 96 (1975) [Zh. Eksp. Teor. Fiz. Pis'ma Red. **21**, 216 (1975)]
¹² I. O. Kulik, A. N. Omel'yanchuk, Sov. J. Low Temp. Phys. **4**, 142 (1978) [Fiz. Nizk. Temp. **3**, 459 (1977)]
¹³ W. Haberkorn, H. Knauer, and J. Richter, phys. stat. sol. (a) **47**, K161 (1978)
¹⁴ E. D. McCumber, J. Appl. Phys. **39**, 3113 (1968)
¹⁵ W. C. Stewart, Appl. Phys. Lett. **12**, 277 (1968)
¹⁶ T. A. Fulton and L. N. Dunkleberger, Phys. Rev. **B 11**, 4760 (1974)
¹⁷ R. F. Voss and R. A. Webb, Phys. Rev. Lett. **47**, 265 (1981)
¹⁸ S. Washburn, R. A. Webb, R. F. Voss, and S. M. Faris, Phys. Rev. Lett. **54**, 2712 (1985)
¹⁹ J. M. Martinis, M. H. Devoret, and J. Clarke, Phys. Rev. Lett. **55**, 1543 (1985)
²⁰ A. Schmid, Phys. Rev. Lett. **51**, 1506 (1983)
²¹ V. Ambegaokar and B. I. Halperin, Phys. Rev. Lett. **22**, 1364 (1969)
²² A. O. Caldeira and A. J. Leggett, Ann. Phys. **149**, 374 (1983)
²³ A. I. Larkin, K. K. Likharev, and Yu. N. Ovchinnikov Physica **126 B**, 414 (1984)
²⁴ M. Tinkham, *Introduction to superconductivity*, (McGraw - Hill Kogakusha Ltd., Tokyo, 1975) pp. 230
²⁵ K. K. Likharev and A. B. Zorin, J. Low Temp. Phys. **59**, 347 (1985); D. V. Averin, A. B. Zorin, and K. K. Likharev, Sov. Phys. JETP **88**, 407 (1985) [Zh. Eksp. Teor. Fiz. **88**, 692 (1985)]
²⁶ G. Schön and A. D. Zaikin, Phys. Rep. **5&6**, 237 (1990)
²⁷ L. S. Kuzmin and D. B. Haviland, Phys. Rev. Lett. **67**, 2890 (1991); D. B. Haviland, L. S. Kuzmin, P. Delsing, K. K. Likharev, and T. Claeson, Z. Phys. B - Condensed Matter **85**, 339 (1991)
²⁸ G. E. Blonder, M. Tinkham, and T. M. Klapwijk, Phys. Rev. **B 25**, 4515 (1982)
²⁹ S. N. Artemenko, A. F. Volkov, and A. V. Zaitsev, Sov. Phys. JETP **49**, 924 (1979) [Th. Eksp. Teor. Fiz. **76**, 1816 (1979)]

- ³⁰ A. Pleceník, M. Grajcar, Š. Beňačka, P. Seidel, and A. Pfuch, Phys. Rev. **B 49**, 10016 (1994)
- ³¹ K. Gloos and F. Martin, Z. Phys. B - Condensed Matter **99**, 321 (1996)
- ³² Yu. V. Sharvin, Sov. Phys. JETP **21**, 655 (1965) [Zh. Eksp. Teor. Fiz. **48**, 984 (1965)]
- ³³ P. Delsing, K. K. Likharev, L. S. Kuzmin, and T. Claeson, Phys. Rev. Lett. **63**, 1180 (1989)
- ³⁴ K. Flensberg, S. M. Girin, M. Jonson, D. P. Penn and M. D. Stiles, Z. Phys. B - Condensed Matter **85**, 395 (1991)
- ³⁵ P. Wahlgren, P. Delsing, and D. B. Haviland, Phys. Rev. **B 52**, 2293 (1995)
- ³⁶ K. P. Hirvi, J. P. Kauppinen, A. N. Korotkov, M. A. Paalanen, and J. P. Pekola, Czech. J. Phys. **46**, 3345 (1997)
- ³⁷ Yu. Nazarov, Sov. Phys. JETP **68**, 561 (1989) [Zh. Eksp. Teor. Fiz. **95**, 975 (1989)]
- ³⁸ Albert Messiah, *Quantenmechanik*, (Walter de Gruyter, Berlin, New York 1979), Vol. 2, pp. 429; [Mécanique Quantique, Vol. 2, (Dunod, Editeur, Paris 1964)]
- ³⁹ E. Scheer, P. Joyez, D. Esteve, C. Urbina, and M. H. Devoret, Phys. Rev. Lett. **78**, 3535 (1997)
- ⁴⁰ K. K. Likharev, Rev. Mod. Phys. **51**, 101 (1979)